

We thank the anonymous reviewers for their useful comments and suggestions. We present the reviewers' comments in bold and our responses in standard font. For clarity, in our responses we refer to the new figure numbers, which have changed with the addition of the new Figures 1 and 2.

Given the nature of the comments from Reviewer #1 (i.e. more essay-style than point-by-point), it seems most appropriate to respond by summarising the changes we have made at the end of the comments, rather than throughout. There are also two specific points along the way, which we have responded to individually. Reviewer #2's comments are addressed point-by-point, and Reviewer #3's comments are addressed in the responses to the other two reviewers.

Anonymous Referee #1

The manuscript describes aircraft and radar observations in a line of small cumulus with bases at about +11 C and tops around -15 C. This review focuses on observations from the BAE-146 measurements in relatively new, isolated updrafts that have not been contaminated with ice from older convection.

The main point that needs to be corrected is that the manuscript consistently and persistently attributes high ice concentrations observed in the -3 to -8 C region to the Hallett-Mossop (H-M) secondary ice formation process. In several places the manuscript states that there are sufficient drops smaller than 13 microns and larger than 24 microns in the presence of graupel between -3 and -8 C, and then attributes measurements of relatively high ice concentrations to the H-M process. The manuscript goes on to make the case that the H-M process supplies ice splinters that freeze the remaining supercooled drops. However, the observations do not provide confirmatory evidence for the conclusion that the H-M process is actually operating.

The observations demonstrate the following:

- 1. H-M conditions are met in certain regions of clouds.**
- 2. Relatively high ice concentrations are observed**
- 3. Ice crystal habits are typical of growth in the temperature range from – 3 to – 8 C.**
- 4. Large supercooled (drizzle and rain) drops appear to freeze before smaller cloud drops freeze.**

From these observations the manuscript concludes that the H-M process is responsible for producing small ice splinters that then collide with and freeze the large supercooled drops. While the H-M mechanism could be responsible for the production of small ice and subsequent freezing of larger supercooled drops, it is not the only process that could be responsible. Secondary ice production in actual clouds is not well understood and not well quantified. The manuscript tends to build its case on circumstantial and sometimes facial evidence. For example, the production of small ice via drop freezing, spicule formation and ejection of small ice is another mechanism (demonstrated in the laboratory by Thomas Leisner). However, this mechanism is dismissed in the manuscript via the following discussion:

Lawson et al. (2015) stated that the presence of drops larger than 200 microns in updrafts At – 6 C was required for significant ice enhancements by droplet fragmentation.

The actual verbiage from Lawson et al. (2015) is:

"Model runs were also conducted by varying the initialized DSD and the initial ice PSD. If the DSD at -6 C does not contain drops larger than about 200 micron in diameter, the conversion to ice via drop-freezing secondary ice production and riming is greatly diminished, resulting in less ice and more supercooled water being transported higher in the cloud."

The manuscript has taken the results from a cloud model used as an aid in the interpretation of the observations and implied that the Lawson et al. (2015) stated a conclusion. This is very inappropriate and misleading.

The manuscript goes on to state:

"The mean concentrations of N_{Round} > 200 _m in updrafts in runs 11.1, 11.4 and 13 were 0, 3.6 and 0.9 /L respectively. The average number of fragments expected from a 200 micron drop is 0.04 (Lawson et al., 2015, Fig. 12), meaning if all these drops were to freeze in the H–M zone only a minimal enhancement would be expected."

This is a misinterpretation of Fig. 12, which shows statistically the number of fragments a drop would produce based on the model results. Because this is a statistical result, the proper interpretation is that statistically, the model predicts that one in every 25 drops that are 200 microns in diameter will produce an ice particle. However, this is a cascading process, whereby this ice particle could freeze a 2^{avour2tre}-diameter drop that could produce hundreds of ice particles, and so on, producing rapid glaciation. The statement in Lawson et al. (2015) is sharing a generalized result form the model and this not sufficient justification to eliminate one secondary ice process in 2^{avour} of another.

It is not clear from reading Lawson et al. (2015) that this work is simply to aid the interpretation of observations- the modelling work is presented on the same footing as the observations, and was tuned to their observations. Furthermore, to our knowledge it is the only work to date to attempt to quantify the droplet freezing secondary ice production mechanism(s) in any usable fashion. Rather than being "inappropriate and misleading", the comparison was made in good faith, to give the reader an indication that the warm rain process in our study was much less active than in Lawson et al. To satisfy the reviewer's concerns, we have removed any calculations using Lawson et al, and have made the argument more qualitative, to say that based on the differences in the warm rain process, we expect drop freezing secondary ice to be less effective than in Lawson et al, but to be more quantitative you would need to use a model.

"Modelling work by Lawson et al. (2015) suggested that the concentration of drops larger than 200 μm in updrafts at -6°C was an indicator for whether significant ice enhancements by droplet fragmentation would occur. The mean concentrations of $N_{\text{Round}} > 200 \mu\text{m}$ in updrafts in runs 11.1, 11.4 and 13 were 0, 3.6 and 0.9 L^{-1} respectively. Based on our observations alone we are not able to quantitatively assess the potential of droplet freezing secondary ice formation to affect ice concentrations, but these numbers will serve as a reference point for microphysical simulations which are beyond the scope of this paper. Using our observations of frozen drops and a comparison between our droplet size distributions and the observations and modelling work by Lawson et al. (2015), we are able to say that secondary ice formation associated with droplet freezing is likely to

have been active in our case study, but to a lesser extent than in the tropical chimney clouds described by Lawson et al. (2015). The cooler cloud base in our case study means the drops were generally smaller when reaching freezing temperatures, and therefore less efficient at secondary ice production when freezing.”

This reviewer is not saying that the H-M process was not operating in the subject clouds, that the spicule/ice production process was operating, or that some other (perhaps unknown) secondary ice process was or was not operating. The point is that there is not enough evidence to come to the conclusion that H-M was responsible for the relatively high ice concentrations. The conclusions are built on a house of cards.

For example, from the manuscript: “The crystal habits and ice concentrations of hundreds per litre make it clear that these particles were generated by the H-M process, and were lifted further up in the cloud by updrafts.” This statement cannot be proved. What the observations do indicate is that ice with habits characteristic of a certain temperature range were measured in concentrations of hundreds per liter and observed in colder (higher) regions of the cloud.

The manuscript needs to be significantly modified so that the H-M process is not “promoted”. Instead, the observations should be presented, the interpretation that the measured ice concentration far exceeds what is expected from primary nucleation, and that a secondary ice process may be responsible for the high ice concentrations. If desired, the manuscript could then list some candidate processes (e.g., H-M, spicule formation, drop fragmentation, crystal-crystal shattering, etc.), and also state that the basic H-M conditions are met in and near the regions where the high ice is observed. But there is not enough evidence to conclude that the H-M process is responsible. It is also inaccurate to state that the spicule ice formation process is not responsible for the high ice concentrations, because not enough is known about that process. Observational scientific papers should present the data and offer interpretations, not piece together circumstantial evidence in an effort to come up with an explanation.

There are also several minor issues that need to be addressed in the paper. For example, the Abstract overstates the certainty of existence of the H-M process:

“It is therefore clear that the freezing of supercooled drizzle drops not only provides a pathway to advance the onset of the H-M process, it also accelerates glaciation and the formation of precipitation once it has begun.”

The observational evidence indicates that the measurements of ice concentration in the – 3 to – 8 C temperature range (i.e. the H-M region) greatly exceed those expected from primary nucleation. However, the manuscript states that freezing of supercooled drizzle provides a pathway to advance the onset of the H-M process, which is an implicit confirmation that the H-M process is responsible for the increased ice concentration. There is no direct evidence that the H-M process is actually operating, only circumstantial evidence, so these types of implicit confirmations of the H-M process need to be eliminated.

Another example: The manuscript cites the Harris-Hobbs and Cooper (1987) technique for estimating the number of ice particles produced by the H-M process. However, this approach,

while appropriate in its day, uses 30-year old technology, including optical probes without anti-shattering tips, and the results are not applicable today.

Although the reviewer is correct to say measurement technology has improved in the last 30 years, the approach of Harris-Hobbs and Cooper (1987) is a calculation using the ice size distribution. The calculation itself (i.e. the equation) is just as valid as it was 30 years ago. We have removed any comparison of the numbers from the older papers without anti-shatter tips. The technique is now used solely on our data, which is self-consistent.

This reviewer cannot recommend publication until the major issue, overly promoting the role of the H-M process, which is described in detail in this review, is rectified. The paper needs to focus on the observations, not the H-M process, which is mentioned 57 times in the manuscript. This reviewer recommends that the manuscript be revised to:

- 1) compare the observations to ice concentrations expected from primary nucleation,**
- 2) point out that the ice concentration measurements far exceed those expected from primary nucleation,**
- 3) show how the role of freezing of supercooled drizzle may play a role,**
- 4) explore the possibility that there is an active secondary ice production process active, and**
- 5) point out that the ice number concentration enhancement falls within the conditions defined by the H-M mechanism and that H-M is one of the possible candidates.**

General response to comments from Reviewer #1

We thank the reviewer for their useful critique. We have made a number of changes to the manuscript based on Reviewer #1's comments (and some from the other two reviewers). In particular, the discussion section has been rewritten and the conclusions and abstract edited accordingly. The results and discussion regarding ice formation have been rewritten as follows:

Sections 3.2 & 3.3: Description of measurements on a run-by-run basis, as before

Section 3.4: Summary of measurements, including comparison to IN calculations from DeMott et al. (2010), highlighting the transition from primary to secondary ice and the measurement of frozen drops followed by vapour-grown ice, predominantly with columnar features. This section includes some parts that formed part of the discussion in the ACPD version.

Section 4.3 then discusses what we may learn from the observations of:

4.3.1: Columns and mixed-habit ice: There is a secondary ice production mechanism active at temperatures where columns are the primary ice habit, and these ice crystals are also sent to different regions of the cloud.

4.3.2 Frozen drops: There is a source of small ice crystals that impact upon drizzle drops to freeze them, but are otherwise too small to see until they have grown by vapour diffusion, which takes time.

These two sections, as well as parts of the results section, invoke the concept of secondary ice production, but all discussion of the different ice multiplication mechanisms (H-M, drop freezing and

ice-ice collisions) are now contained in Section 4.3.3 in the discussion. Regarding drop-freezing secondary ice production, we have stated that it's likely to be less effective than in Lawson et al (2015) due to the colder cloud base in our study, but we can't rule it out. It is likely to have been active in some form, but full quantification is not possible without a microphysics model which includes all the processes.

The abstract and conclusions have also been rewritten to take into account the above. The main take-home message is now that there seems to be one or more source(s) of small ice crystals that freeze the drops, which then grow large and precipitate out.

Anonymous Referee #2

Review of "Observations of cloud microphysics and ice formation during COPE" by Taylor et al.

Recommendation: Requires revision before acceptance in ACP.

This study examines data collected in two lines of cumulus clouds over the Southwest Peninsula of the UK acquired during COPE. Sampling was performed first along a line of closely packed cells, followed by repeated penetrations through an isolated cell as it grew and became glaciated. The evolution of the observed cloud and aerosol properties is explained in terms of the action of the Hallett-Mossop process. The continued passes through the developing cumulus cell are especially unique, and hence should indeed be published. However, I find that some of the writing in the paper is not precise, overly speculative, and not totally justified by the presented data. In particular, the authors state that the observations show that the H-M process was initiated from the recirculated ice, with ice splinters causing the drizzle drops to freeze on contact, forming additional instant-rimers. Although it could be argued that the results presented in the paper are consistent with this explanation, there could also be other mechanisms acting that could also have explained the observations. Thus, I recommend that the writing in the paper be carefully examined to note what trends are consistent with the H-M process, rather than stating that the H-M process explains the results. There are also a number of locations in the paper where the writing could be made more precise and quantitative, with the numbers of speculative comments reduced. This is further explained below in the context of some passages of the manuscript.

We thank the reviewer for their detailed comments, which we respond to point-by-point. The question of "trends are consistent with the H-M process, rather than stating that the H-M process explains the results" has been addressed in the changes to the discussion section outlined in the responses to Reviewer #1.

A second major point relates to questions about some of the microphysical analysis that is presented in the paper. It seems that there is an overreliance on the images from the 2DC/CIP for identification of the phases of the particles, and that other information should be additional considered. The definitions of circularity and roundness are important for many of the results that are presented in the paper. With this in mind, I think that the definition of circularity should be stated in the manuscript. Also, how sensitive are your results to the definitions of low, medium and high irregularity and roundness? If a minor adjustment is made in the threshold to change these classifications are your results significantly impacted?

The definitions of circularity are listed in appendix A1. To show the sensitivity to the exact circularity thresholds, we have added the line

"Varying the circularity thresholds (in all categories concurrently) by ± 0.05 caused a 5 – 20 % change in the ice and round concentrations reported by the 2DS."

More importantly, I am surprised that a lot of the shape analysis in the manuscript is based on the 2DS images rather than the CPI images which give more detailed pictures and would allow the riming to be much more easily determined.

As stated on pages 16056-7 “Quantitative hydrometeor concentrations could not be determined from the CPI during COPE” The sample volume of the CPI is much smaller than the 2DS, and it suffers from very poor counting statistics in short penetrations through mixed-phase clouds. For example, in a cloud pass where the 2DS recorded thousands of cloud drops and hundreds of ice particles, the CPI might record just 30 cloud drops and no ice. The concentrations determined by the 2DS are therefore much more quantitative. The 2DS is a well-established cloud probe and has been used successfully in many previous studies (e.g. Crosier et al., 2011; Lawson et al., 2015; Lloyd et al., 2014)

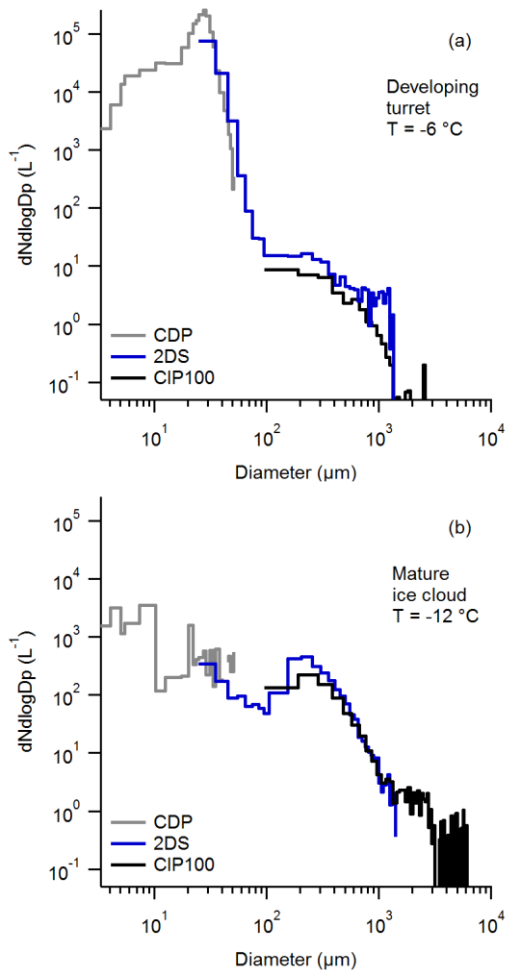
I also have difficulty in understanding why particles that occurred on the edges of the photodiode array would be any different than those occurring in other portions of the photodiode array: you are sampling the same population of particles so why would they be any less likely to be mixed-phase?

Cloud phase is often size-dependent, for example a mixed-phase cloud made up of 30 μm drops and 500 μm graupel. Also, larger particles are more likely to fall on the edge of the array. In practice, this means the edge particles are often either ice or liquid, rather than a mix of the two. This may not be true in other environments (such as clouds in which larger rain drops are more numerous) but it was the case in COPE. There is no perfect solution for how to deal with edge particles on which standard shape analysis cannot be performed, but this solution worked well for this dataset.

No size distributions are presented in the manuscript. How well do the 2DS and CIP distributions agree? How well does the CDP distribution agree with that of the 2DS in the overlap range? Answering these questions would help justify the robustness of the data.

We have added in the following as a new figure to the experimental section

“A comparison of example size distributions measured by the three probes is presented in Fig. 1, which shows broad agreement between the probes where their size ranges overlap.



Comparison of size distributions from the CDP, 2DS and CIP100 probes during selected cloud penetrations through (a) a developing turret and (b) a mature glaciated region. The first 2 size bins from the 2DS and CIP100 were removed, as they are subject to large uncertainty, and are not used in this analysis."

And, finally, I have some questions about the phase identification analysis. It would seem that there would be some additional information that might help better determine the phase, especially given the out of focus 2DS images that are used in some of the analysis. For example, was the shape of the CDP distributions examined? They tend to be more peaked in liquid clouds and flatter in ice clouds.

The CDP measures particles in the size range 2 – 50 μm whereas the 2DS HI, MI and LI categories are for particles larger than $\sim 90 \mu\text{m}$. Cloud drops can coincide with larger ice particles- the clouds sampled in this analysis were predominantly mixed-phase. As shown in the figure above, the CDP distributions did tend to be monomodal in liquid clouds, but flatter and in far lower concentrations in ice cloud. This doesn't really add to the analysis though. The best measure of the cloud phase is by comparing the concentrations of cloud drops measured by the CDP and drizzle and ice measured by the 2DS.

Other questions include the following: was the H or V channel of the 2DS used, or some combination?

We have added to appendix A1:

"The 2DS has two data channels measured by vertically- and horizontally-aligned detectors. We combined images from channels to calculate an average concentration. This technique improves the counting statistics in low concentrations, as the large majority of particles are observed only on a single channel."

Were depth of field corrections applied for the small particles?

We have added to appendix A1:

"The sample volume was calculated using the measured airspeed and size-dependent sample area, as described by Heymsfield and Parrish (1978)."

It is stated that varying the inter-arrival time threshold had little impact on the derived concentrations and that a constant threshold was used: although this would be problematic in conditions of large or heavy ice, this seems reasonable for the conditions sampled. Nevertheless, it would be nice to know quantitatively what "little" effect means: 10% or a factor of 2? And, is there any way to be more quantitative about the amount of riming that is occurring?

We have added to the appendix:

"Using either no IAT threshold, or a threshold of 2×10^{-6} s, caused a 5 – 15% increase, or decrease respectively, in the ice and round concentrations reported by the 2DS."

I find the naming of the runs (e.g., 10.3.1, and 11.1) rather strange. Can the runs simply be designated by their times, or is there something more significant about these naming conventions that is used. If they are named by time or altitude, it would help give me a perspective of when/where they were.

In the archived flight logs, runs are labelled as run 10, run 11, run 12 etc so it's good practice to keep the labelling consistent with those. The numbers after the decimal points are there to signify that it is only part of one of the runs in the flight logs.

The caption to table 2 now has the sentence added:

"The run numbers correspond to full or sections of labelled runs in the archived flight logs."

To simplify things slightly, run 10.3.1 has been renamed to 10.3

I think some of the figures could be better presented to give a better perspective of where the data were obtained to help interpret the patterns within them. For example, in Figure 5 can the concentration plots be on the left hand side of the plot and the vertical velocities on the right hand side of the plot? Then the plots could be sorted vertically by altitude giving a better graphical manner to interpret the variations between the runs.

There's a lot of information plotted on Figure 7, and it went through several iterations during the drafting process, one of which was very similar to what the reviewer describes. In that configuration, the spatial link between the concentrations and the vertical wind is lost. The way it is currently

plotted, the runs are still sorted by altitude, but just in 2 columns. This seemed to be the best compromise.

Abstract: I think the abstract should be considerably tightened and made more quantitative, stating what the observations were with a minimal focus on speculative comments explaining the observations.

The abstract has been largely rewritten to focus on the observations.

In addition, there is too much introductory material in the abstract that should be removed (e.g., the first two sentences are fine for an introduction, but not needed in the abstract). That would allow extra space so that it could be explicitly stated what conditions were present to justify statement that conditions of H-M process were met.

We have removed the introductory sentences, but also reference to H-M as it has been moved to later in the abstract.

In the third paragraph, the statement of “a few drizzle drops” should be made more quantitative.

We have changed it to say “drizzle concentrations increased from $\sim 0.5 \text{ L}^{-1}$ up to $\sim 20 \text{ L}^{-1}$ in around twenty minutes. Ice concentrations developed up to a few per litre, which is around the level expected of primary IN.”

Also, it could be noted that graupel formed after the drizzle drops, but the freezing of the drizzle to form graupel was not explicitly observed.

It now says

“The ice images were most consistent with freezing drizzle, rather than smaller cloud drops or interstitial IN forming the first ice.”

In the fourth paragraph it is stated that ice splinters were captured by supercooled drizzle drops causing them to freeze: but, again this was not a process that was observed so more quantitative comments about what was actually observed shoud be noted. In the fifth paragraph, can you stated what quantitatively a “majority of precipitation-sized particles” means. The second to last sentence in the abstract is consistent with the observations, but is not necessarily the only explanation for the observations and hence this statement should be reworded.

We have reworded these two paragraphs:

“Almost all of the initial secondary ice particles were frozen drops, while vapour-grown ice crystals were dominant in the latter stages. Our observations are consistent with the production of large numbers of small secondary ice crystals/fragments, by a mechanism such as Hallett-Mossop or droplets shattering upon freezing. Some of the small ice froze drizzle drops on contact, while others grew more slowly by vapour deposition. Graupel and columns were seen in cloud penetrations up to the -12°C level, though many ice particles were mixed-habit due to riming and growth by vapour deposition at multiple temperatures.

Our observations demonstrate that the freezing of drizzle/raindrops is an important process that dominates the formation of large ice in the intermediate stages of cloud development. As these frozen drops were the first precipitation observed, it is clear that interactions between the warm rain and secondary ice production processes are key to determining the timing and location of precipitation."

Page 16054, line 10: Why was this particular case (3 August) chosen for analysis? A couple of sentences of explanation should be given.

We have added "...as it presented the most detailed set of observations, including repeated aircraft penetrations through cloud regions with prolific ice production"

Page 16060, line 11: Was there any evolution of the altitude of the cloud base during the height?

There may have been but we are not able to assess this with our observations. The text already states that the cloud base was similar to 1km, not exactly 1km.

Page 16061, line 3-4: Could there have been any possibility of APIPs from the King Air that could have generated ice, ultimately affecting the measurements from the BaE- 146?

This seems unlikely. Most of the time the two aircraft were sampling different clouds. Similar cloud formation and progression (i.e. rising turrets and increasing reflectivity) was observed by the ground radar in clouds that the aircraft did not fly in. If the aircraft injected significant ice into the clouds, these clouds would be expected to develop and precipitate faster than other clouds, which was not the case.

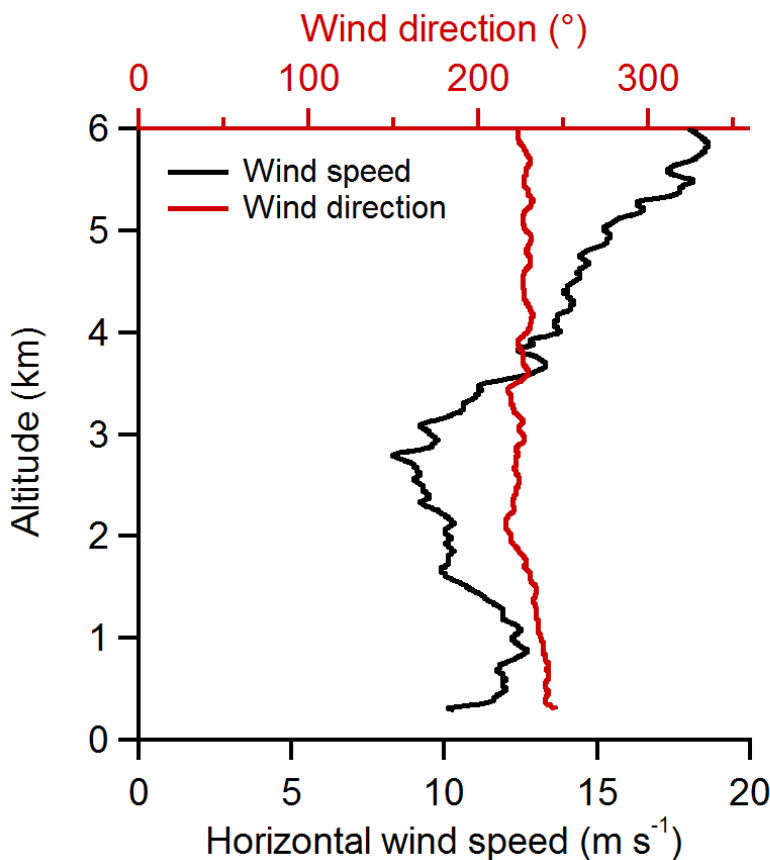
Page 16062, line 9: What do you mean by three runs? I only see a single line in Figure 3 so I am wondering how you define a run.

The line referring to this figure (now Figure 5) says "Figure 5 shows in situ microphysical data recorded during one of these runs" so it is clear that only one run is presented. Data from the other two longitudinal runs did not add anything further to the analysis so are not presented in the manuscript.

Page 16062, line 10: There were several times in the paper I was wanting to see a vertical profile of the wind. Could you show one?

We have added the following plot to the start of the results section

"Figure 2 shows the vertical profile of wind speed and direction. The wind direction was southwesterly and showed little variation with altitude. The wind speed was $8 - 13 \text{ ms}^{-1}$ up to 3 km, then increased with height to reach 19 ms^{-1} by 5.8 km.



Vertical profile of horizontal wind speed and direction measured from the 1500 UTC radiosonde launched from Davidstow, the same location as the NCAS precipitation radar.”

Page 16062, first paragraph in Section 3.2: Is it possible to also include a plot of the liquid fraction? I think that would be very useful for many of the analysis fields that you presented.

For the liquid fraction, there is no single answer. For example, both the liquid and ice number and mass fractions are very size-dependent. The best way to tell is to compare the CDP concentration and/or LWC to the ice and drizzle concentrations measured by the 2DS, which are already plotted.

Are the components of ice included or not included in the calculation of effective radius? It would seem important to exclude them for calculating the effective radius.

It was included, we have clarified by redefining it as R_{32}

“The variable R_{32} in Fig. 5 is defined as the ratio of the third to the second moment of the hydrometeor size distribution generated by combining all-accept data from the CDP, 2DS and CIP100. For spherical drops, this is the same as the effective radius; when used in clouds containing nonspherical particles it is a useful indicator of the average particle size.”

This definition is sufficient as R_{32} is not used quantitatively (e.g. to compare to remote sensing measurements), but as an indicator of particle size.

Page 16062, line 26 (also several other points in paper): I have trouble seeing where you are getting the information about the spatial scale of the vertical motion from. Was some sort of FFT analysis applied? Or what else was done to determine the spatial scale of the vertical motion?

It's just from looking at figure 5c and seeing how wide the up/downdrafts are.

Page 16063, line 11: Could look at shape of CDP to verify that the cloud was almost exclusively composed of liquid drops?

The text refers to a measured CDP concentration of 200 cm^{-3} . If this was all ice, the concentration would be three orders of magnitude higher than typical ice concentrations in mature ice clouds.

Page 16063, line 15: It would be interesting to show the size distributions to better visualize these comments on the contributions of drops with different diameters.

The relevant part of the new discussions section (in 4.3.3) now refers to the new figure 1 which shows a size distribution

Page 16064, paragraph on Region II: I'm not convinced that I see evidence of liquid water from the images that are presented for Region II. It is claimed that this is a more mature cloud because of the presence of the ice crystals.

We have stated in the experimental section that the LWC is measured by the CDP, and

"...agreed with the onboard Johnson–Williams hotwire probe within ~12% below $\sim 0.9 \text{ gm}^{-3}$ (on the CDP), above which the hotwire probe began to saturate. The reported LWC values are from the CDP, as the hotwire probe suffered from wetting and saturation artefacts"

Additionally, the measured CDP number concentration was $60/\text{cm}^3$, and there is no known mechanism to generate such a high concentration of small ice in atmospheric clouds.

Is there some way that is more objective that can be used to estimate the age of the cloud to make the analysis more objective?

We've added in

"Regions I – III were parts of the line that had emerged 30 mins earlier, but was still active dynamically, with new cells emerging on the edges of pre-existing cloud regions. Regions IV and V were further downwind in a region that originated around an hour earlier, passed through a dynamically active phase and was now quiescent and stratiform."

And also about region V

"Following the aircraft penetration, these new updrafts developed into a reinvigorated dynamic cloud system."

Given the spatial and temporal resolution of the radar, it's very difficult to be more precise than this.

Page 16064, line 13: Are some of the donut type crystals seen in region III assumed to be liquid particles? Out of focus ice particles can appear as round donuts in 2DS/CIP images, so it is not necessary that these particles are liquid.

No the liquid was measured by the CDP, the figure shows the 2DS only measured a few per litre in region III.

Page 16064, line 17: See my comments on microphysics analysis. How well do you really know what the concentrations of graupel or round particles are? What is their uncertainty based on the shape analysis?

This is now addressed in appendix A1, see previous comment about varying the circularity thresholds

Page 16064, discussion of Region III: Inevitably, you may be seeing some differences in the regions from what part of the cell was penetrated (edges or cores). This is certainly acknowledged in the text, but I am left wondering to what degree some of your conclusions can be affected by these differences.

The text already states

"in some of the cloud penetrations, particularly the later penetrations where the cloud was more developed and reflectivity was higher, the LWC and updraft strength may be biased low compared to the updraft cores."

which is fairly clear. Also, near the start of section 3.3.2 we have added

"Some variation in maturity of cloud regions, and concentrations within those regions, is to be expected due to penetrations through different parts of the cloud, but the general progression from young liquid cloud to mature ice cloud was still clear, as was the timescale over which this transition took place."

Page 16065, line 8: I would recommend removing the last sentence of this paragraph unless something more concrete can be said rather than the speculative statement.

Done

Page 16065, line 11: Is it differences in ages, or do what extend could some of these differences be associated with where in the cells the penetrations are made? Do you see any gradual maturation of the cells on the radar that can be quantified?

We have added to the start of section 3.2

"The ground-based precipitation radar observed newly-formed cloud regions increasing in height and reflectivity as they matured and moved downwind. The timescale from initiation, development of precipitation and dissipation was of the order of one hour, though mixing between different cloud regions meant the precise age of any one region was often difficult to determine."

Page 16065, line 25-26: I think it would be more fair to say that your results are consistent with the action of the H-M process: it does not really infer that this process is going on.

We have phrased the rewritten discussion section in this way

Page 16066, line 3: Where does this 4 km come from? It seems to be more than 4 km away from the other cells on this figure.

Reading off figure 5 it's 4.7 km, so it has been changed to ~5 km

Page 16066, line 14: can you quantify what you mean by relatively low?

We've added that it was below -5 dBZ

Page 16066, line 16: Are these numbers correct? The 0.5 m^{-3} of 1 mm drops seems a little high for this reflectivity.

The numbers are correct. To clarify and give a better feel of the numbers, we have changed the text to

"For comparison, the peak reflectivity of -3 dBZ is equivalent to a concentration of 0.5 m^{-3} of 1 mm raindrops , 500 L^{-1} of $100 \mu\text{m}$ drops, or 2000 cm^{-3} of $25 \mu\text{m}$ drops"

Page 16067, line 17: Can you say something more quantitative than young clouds?

The text refers to figure 5 showing Run 11.2. We have added to the discussion in section 3.2:

"Regions I – III were parts of the line that had emerged 30 mins earlier, but was still active dynamically, with new cells emerging on the edges of pre-existing cloud regions. Regions IV and V were further downwind in a region that originated around an hour earlier, passed through a dynamically active phase but was now quiescent and stratiform"

Page 16068, line 10: I find this hard to justify with presented data because so many of the images are out of focus.

The text says

"As a general trend, in the earlier, lower altitude runs, the cloud was composed almost entirely of liquid cloud drops, and the peak LWC increased with altitude. This trend proceeded until significant precipitation was observed, at which point the LWC began to decrease, likely by scavenging and entrainment. At increasing altitude/time, the cloud shifted to mixed-phase and finally was nearly glaciated in the final run."

The liquid drops were mainly cloud drops measured by the CDP, which does not have such ambiguities.

Page 16068, line 18: Can something more quantitative be stated to show that the downwind updraft region was more turbulent?

This now reads

"In Run 11.1, the downwind updraft region was more turbulent, with vertical velocity varying on the scale of tens of metres, where the upwind updraft was 300m wide"

Page 16069, line 10 and after: Can you refer to which particular figure you are seeing this information about the particle characteristics? I'm not convinced that you really have the resolution in the particle images to observe this. So many particles on the CIP/2DS don't really have sufficient resolution. Can't you be using the CPI and showing specific images to show that this is occurring?

We have already discussed the fact the CPI did not record very many particles due to its low sample volume. Example images we are referring to are now highlighted in figures 8 and 9 with red arrows

Page 16069. line 22: What is the basis of saying that the downwind side is more turbulent?

The upwind side consists of two broad updraft sections, 800 and 1000m across, whereas the downwind side has several up/downdrafts each 50-250m across. This is visible on figure 7

Page 16070, line 8: You can say frozen drops but not recently frozen drops. There is nothing in the observations that says the time at which the drops were frozen.

The text now reads

“...a mixture of small columns, recently frozen drops and rimed ice. The frozen drops had some riming but were still recognisable as frozen drops, so are likely to have frozen fairly recently.”

Page 16070, line 18: Remember that you are not necessarily sampling the exact same locations in the cloud. Plus with the evolution and movement of particles, you can't necessarily equate one part of the cloud to the other. Thus, some of the discussion should be adjusted accordingly.

Please see earlier comment regarding this question

Page 16071, line 17: reword “following cloud upwind”. I think I know what you mean, but this is worded awkwardly.

The subsection title is now “Ice in the next cloud upwind” and the paragraph says “...the BAe-146 made three runs near the top of the next cloud to the southwest along line CD (i.e. upwind)”

Page 16072, paragraph beginning line 3: A lot of the comments in this paragraph are overly speculative (suggesting, likely, may have, etc.). I think it would be better to say the data are consistent with these processes. Are there any more processes that the data are also consistent with?

We have rewritten the discussion section to consider other processes that may explain our results.

Page 16072, line 23: Emphasize that the results are consistent with some processes, state if there are any other processes that should also explain the results, and note that there really is nothing that proves what is stated.

This has been taken into account when rewriting the discussion section

Page 16073, Section 4.1: Is this section really needed? I think the earlier reference in the paper to the 2004 floods should be sufficient.

The section is useful as a comparison of the similarities and differences between this case study and the Boscastle event, which was one of the main motivations for the project. They were similar, but not the same, and it is useful to explicitly point this out. It helps provide some context e.g. for modellers also looking at this case study

Page 16074, line 13: It would be nice to show the wind gradient or vertical shear in the paper somewhere.

We've added a reference to the new figure 2 showing the wind vertical profile

Page 16076, line 6: It should be emphasized that it takes time for any ice crystal produced at cloud top to fall to the measurement level, so the approach discussed here should provide a maximum estimate of the ice crystal concentration.

We've added that to the previous paragraph

Page 16077, line 11: Can you be more quantitative rather than use words such as minimal?

This has been removed in the restructuring/rewriting of the discussion section

Page 16078, line 2: I would argue that this is a possible explanation or that the results are consistent with this explanation.

The comment refers to ice seeding from pre-existing cloud layers aloft. We have already ruled this out in the section on primary ice

"the cloud region that was the focus of this analysis was initially isolated from neighbouring clouds by several kilometres, and no aerosol layers or regions containing outflow from previous clouds were detected in the immediate vicinity."

Page 16078, line 3: classified rather than classed

This has been removed in the restructuring/rewriting of the discussion section

Page 16078, line 13: Can there be some quantitative analysis presented to justify that ice in the downdraft became more rimed.

It's clear from the images in Figures 8 and 9

Page 16078, line 21: It is not clear these particles were generated by the H-M process, but the results are consistent with their generation by the H-M process.

We have used language like this when rewriting the discussion section

Page 16079, line 8: Remove word "recently"

Done

Page 16808, line 2: I think you determined that the H-M process was consistent with the observations, not necessarily that it was responsible for generating the ice crystal concentrations up to several hundred per liter.

We have taken this into account when rewriting the discussion section

Page 16084, lines 5-12: I don't think this paragraph is needed. I agree that it would be a good subject for a subsequent paper.

It is not strictly necessary for our observations but it helps to place them into the context of the COPE project as a whole (i.e. modelling of this and similar case studies is being undertaken)

Table 2: Is there some significance to the nomenclature that is used to label the runs?

Yes, as discussed above it's the same as the archived flight logs

Figure 1: Can you also show quartiles of the distributions on the plots as well as the individual points in order to give a better idea on what are the trends with respect to altitude?

Quartile statistics vs altitude isn't really an appropriate way to display the trends in the data, which are more temporal than vertical (i.e. cells glaciating as they mature, rather than ice or liquid being in particular levels). For example, consider Run 11.2, shown in Figure 5. This is a run at one altitude, but with very distinct and clear boundaries between liquid clouds (containing very little ice) and ice clouds (containing very little liquid). Averaging over the entire run therefore gives a skewed picture of the data- the average cloud becomes an average of liquid and ice clouds, but doesn't actually look like any real cloud measured.

Figure 3: Shouldn't the upper panel be labeled a, and the other panels subsequently reordered?

Done, and the same for Figure 12.

Figure 4: Should there be a vertical wind field for panel (b) for the first penetration?

Done. The left/right axes of panel (b) have also been swapped as it makes more sense now

Anonymous Referee #3

After careful reading of the manuscript, I saw that already two comments on the paper were posted. I read both of them and found that all questions and other points I would have liked to say are covered by the two reviews, in particular by the second referee. Specifically, I think the authors should take into account his comments with respect to the H-M process and the identification of particle habits using the scheme of Korolev and Sussmann (2000).

So I see no need to repeat the points already made, but like to emphasize my general impression of the manuscript: the topic of the study is of high importance and the measurements (instrumentation and measurement strategy) are impressive. I liked the introductory material a lot since it conveys the relevance of this detailed case study. Further, the data analysis, presentation and discussion are straightforward, the article is well organized and reads smoothly. The figures are clear and appropriate and no redundant material is presented.

In summary, the paper should be published after the revisions recommended above.

We thank the reviewer for their comments. The issues regarding H-M have been addressed in the changes to the discussion, summarised in the response to Reviewer #1.

Regarding the habit classification we have addressed the uncertainties raised by Reviewer #2, adding to the appendix A1

“Varying the circularity thresholds (in all categories concurrently) by ± 0.05 caused a 5 – 20 % change in the ice and round concentrations reported by the 2DS.”

and

“Using either no IAT threshold, or a threshold of 2×10^{-6} s, caused a 5 – 15% increase, or decrease respectively, in the ice and round concentrations reported by the 2DS.”

Observations of cloud microphysics and ice formation during COPE

J. W. Taylor¹, T. W. Choularton¹, A. M. Blyth², Z. Liu¹, K. N. Bower¹,
J. Crosier^{1,3}, M. W. Gallagher¹, P. I. Williams^{1,3}, J. R. Dorsey¹, M. J. Flynn¹,
L. J. Bennett², Y. Huang², J. French⁴, A. Korolev⁵, and P. R. A. Brown⁶

¹Centre for Atmospheric Science, School of Earth, Atmospheric and Environmental Sciences,
University of Manchester, Manchester, UK

²National Centre for Atmospheric Science, University of Leeds, UK

³National Centre for Atmospheric Science, University of Manchester, Manchester, UK

⁴Department of Atmospheric Science, University of Wyoming, Laramie, Wyoming, USA

⁵Cloud Physics and Severe Weather Research Section, Environment Canada, Toronto, Ontario,
Canada

⁶Met Office, Exeter, Devon EX1 3PB, UK

Correspondence to: Jonathan W. Taylor (jonathan.taylor@manchester.ac.uk)

Abstract. ~~Intense rainfall generated by convective clouds causes flash flooding in many parts of the world. Understanding the microphysical processes leading to the formation of precipitation is one of the main challenges to improving our capability to make quantitative precipitation forecasts. Here, We present microphysical observations of cumulus clouds measured over the Southwest Peninsula of~~

5 the UK during the COnvective Precipitation Experiment (COPE) in August 2013, which are framed into a wider context using ground-based and airborne radar measurements. Two lines of cumulus clouds formed in the early afternoon along convergence lines aligned with the peninsula. The lines became longer and broader during the afternoon due to new cell formation and stratiform regions forming downwind of the convective cells. ~~Aircraft penetrations at -5°C showed that in developing regions, all the required conditions of the Hallett-Mossop (H-M) ice multiplication process were met.~~
10 Ice concentrations up to 350 L^{-1} , well in excess of the expected ice nuclei (IN) concentrations, were measured in the mature stratiform regions, indicating that secondary ice production was active.

Detailed sampling focused on an isolated liquid cloud that glaciated as it matured to merge with a band of cloud downwind. In the initial cell, drizzle concentrations increased from $\sim 0.5 \text{ L}^{-1}$ to
15 $\sim 20 \text{ L}^{-1}$ in around twenty minutes. Ice concentrations developed up to a few per litre, which is around the level expected of primary IN. ~~a few drizzle drops were measured, some of which froze to form graupel;~~ The ice images were most consistent with freezing drizzle, rather than smaller cloud drops or interstitial IN forming the first ice.

As new cells emerged in and around the cloud, ice concentrations up to two orders of magnitude
20 higher than the predicted IN concentrations developed, and the cloud glaciated over a period of 12 –

15 minutes. Almost all of the initial secondary ice particles were frozen drops, while vapour-grown ice crystals were dominant in the latter stages. Our observations are consistent with the production of large numbers of small secondary ice crystals/fragments, by a mechanism such as Hallett-Mossop or droplets shattering upon freezing. Some of the small ice froze drizzle drops on contact, while others
25 grew more slowly by vapour deposition. ~~Ice splinters were captured by superecooled drizzle drops causing them to freeze to form instant rimers.~~ Graupel and columns were seen in cloud penetrations up to the -12°C level, though many ice particles were mixed-habit due to riming and growth by vapour deposition at multiple temperatures.

Our observations demonstrate that the freezing of drizzle/raindrops is an important process that
30 dominates the formation of large ice in the intermediate stages of cloud development. As these frozen drops were the first precipitation observed, it is clear that interactions between the warm rain and secondary ice production processes are key to determining the timing and location of precipitation.

~~Frozen drizzle/raindrops initially made up the majority of precipitation-sized particles in the H-M zone, while ice splinters required time to grow by vapour diffusion. It is therefore clear that the~~
35 ~~freezing of superecooled drizzle drops not only provides a pathway to advance the onset of the H-M process, it also accelerates glaciation and the formation of precipitation once it has begun. Accurate representation of both the warm rain and H-M processes, including their interactions with each other and cloud dynamics, appears key to determining the timing and location of precipitation.~~

1 Introduction

40 Extreme rainfall by isolated convective storms can cause flash flooding, leading to property damage and possible loss of life. Short-lived convective storms are thought to be responsible for over half of flash flooding events in the United Kingdom (Hand et al., 2004), and over 3 million properties in England are thought to be at risk of surface flooding (Environment Agency, 2009). The Southwest Peninsula of the UK has a long history of summer flash flooding, with dozens of incidents reported
45 in the last century (Cornwall Council, 2011). The steep, narrow valleys on the north coast of the Southwest Peninsula are particularly vulnerable to flooding as they funnel rainfall down to the sea.

During periods of southwesterly winds, the airstream aligns with the peninsula, and the combination of surface friction and onshore heating drive moist sea breeze fronts inland from both the north and south coasts (Warren et al., 2014). The convergence associated with these opposing fronts creates conditions favourable for convective cloud formation. Similar meteorological phenomena may be found on long, thin peninsulas such as Florida (Burpee, 1979) and the Italian Salento peninsula (Mangia et al., 2004).

In August 2004, particularly destructive flash flooding caused severe damage to the village of Boscastle, and several other villages nearby were also badly affected. A series of convective cells
55 aligned with the southwesterly wind to form a narrow, quasistationary band of precipitation, and up

to 200 mm of rain fell on the surrounding area in around 4 hours (Golding, 2005; Golding et al., 2005). Other notable examples of extreme flash flooding in the area include the ‘Great Flood’ of July 1847, which destroyed several bridges on the River Camel, the Lynmouth flood of 1952 which took 34 lives, and the June 1957 floods in which 200 mm of rain fell in just a few hours.

60 At the time of the August 2004 floods, the UK Met Office’s forecast model grid spacing was 12 km, which was insufficient to resolve the convective cells that formed near Boscastle. The model grid spacing has since been improved to a 1.5 km grid, and higher-resolution hindcasts are able to resolve the August 2004 storms (Golding, 2005). However, quantitative precipitation forecasts remain challenging.

65 Forecasting accuracy is dependent on the successful prediction of the onset, duration, location(s) and intensity of precipitation, which involves a physically-realistic representation of many interacting physical processes. Microphysical processes alone are subject to significant uncertainty. Cloud-resolving models must use parameterisations to predict interactions between different sizes of cloud drops and different types of ice/snow. The use of different microphysical schemes in cloud-resolving
70 models can affect the location, phase and intensity of precipitation (e.g. Loftus and Cotton, 2014; Dasari and Salgado, 2015).

While recent progress has been made in understanding the initiation and development of convective clouds (Browning et al., 2007), and exploring model biases and limitations at different resolutions (Stein et al., 2015), gaining a more detailed understanding of the microphysical processes involved remains a key aspect of improving quantitative precipitation forecasting. Huang et al. (2008) found that in a small sample of clouds formed in similar circumstances, the dominant mechanism leading to the formation of precipitation-sized particles was the accretional growth of graupel. Supercooled raindrops formed by the warm rain process are thought to play an important role in short-circuiting the formation of graupel, hence allowing the more rapid initiation of the Hallett-Mossop
80 (H-M) ice multiplication process (Hallett and Mossop, 1974; Chisnell and Latham, 1976; Phillips et al., 2001; Huang et al., 2008; Sun et al., 2010; Crawford et al., 2012). Several studies have observed such drops in the early stages of convective clouds (e.g. Koenig, 1963; Blyth and Latham, 1993; Rangno and Hobbs, 2005; Lawson et al., 2015), particularly in environments with a warmer cloud base. It is not clear if the supercooled raindrops are the first particles to freeze, or if they collide with primary ice particles produced from frozen cloud drops (e.g. Phillips et al., 2001). On a per-particle basis, larger drops formed by collision-coalescence are more likely to contain ice nuclei (IN) than smaller drops, but they are generally much fewer in number.
85

Raindrops encountering ice splinters ejected by the H-M process can also freeze to become ‘instant-rimers’, meaning the H-M process can progress more quickly than if the splinters had to grow to sizes where they can rime by vapour deposition alone (Chisnell and Latham, 1976). Crawford et al. (2012) found that drizzle drops played an important role in the rapid glaciation of shallow convective clouds, by this process. However, Lawson et al. (2015) recently showed that in cumulus
90

with very active warm-rain processes, fragmentation of freezing drops can also lead to cascading secondary ice production, in the absence of H-M.

95 In this paper, we present observations taken during the COnvective Precipitation Experiment (COPE) which was conducted in the Southwest Peninsula of the UK during July and August 2013 (Blyth et al., 2015; Leon et al., 2015). Measurements of the microphysics, dynamics and thermodynamics were made by two research aircraft, a ground-based precipitation radar, a suite of aerosol instruments and other instrumentation. The principle objective is to document the microphysical 100 observations in sufficient detail to be able to make inferences about the processes occurring in the sampled clouds. This will enable the observations to be used in future work to evaluate the performance of high-resolution numerical models of the clouds and, in particular, the relative importance of resolution and parameterised microphysics in achieving quantitative precipitation forecasts.

First, we examine the horizontal structure and phase of a line of cumulus oriented along the wind 105 direction, formed in similar meteorological conditions to the August 2004 floods. We then present detailed measurements of the development of an initially-isolated cloud as it glaciated. Multiple aircraft penetrations were made through this cloud at increasing altitude as it grew in height, and we 110 present observations showing the conversion of supercooled drizzle drops to graupel ~~via interaction with the H-M process~~. We demonstrate a progression from liquid to ice cloud through mixed-phase stages involving primary graupel, secondary graupel, columns and mixed-habit ice particles. Compared to previous studies, the use of newer instrumentation with more reliable detection of smaller ice particles (Lawson et al., 2006) means we were better able to detect ice closer to where it was produced, and hence may better deduce information on its origins.

2 Experimental

115 2.1 The COPE Project

COPE took place in the Southwest Peninsula of the UK during July – August 2013, and the analysis presented here focuses on one case study from 3rd August, as it presented the most detailed set of observations, including repeated aircraft penetrations through cloud regions with prolific ice 120 production. In situ measurements during COPE were performed using two aircraft platforms- the UK Facility for Airborne Atmospheric Measurement BAe-146 and University of Wyoming King Air 200T (UWKA). Ground-based measurements were performed using the UK National Centre for Atmospheric Science (NCAS) mobile precipitation radar in Davidstow, and an additional site located nearby hosted aerosol instrumentation which was running throughout the whole of the campaign.

The BAe-146 and UWKA aircraft each hosted a suite of in situ probes, providing measurements 125 of size resolved cloud particle number concentration (and to some extent shape) across the entire size range of interest (3 – 6200 µm). The UWKA was also equipped with a Doppler cloud radar, which provided high-resolution vertical profiles mapping the structure of cloud directly above and

below the aircraft. The sampling strategy involved the UWKA flying in and around cloud tops, while the BAe-146 sampled clouds and aerosols at lower levels. The ground-based precipitation radar had
130 a lower spatial resolution than the UWKA cloud radar, but covered a much wider area, and provides the best measure of the horizontal extent and temporal evolution of the clouds.

Both aircraft were fitted with a suite of instrumentation to measure standard data products such as position and velocity, as well as meteorological variables including as temperature, pressure, dew point and liquid water content (LWC). A full summary of instrumentation deployed during COPE is
135 provided by Leon et al. (2015). Here we summarise only the instrumentation used in this analysis.

2.2 BAe-146 instrumentation

2.2.1 Meteorological instrumentation

Ambient air temperature was monitored using de-iced and non-de-iced Rosemount 102 sensors, and here we use the de-iced measurement as most of the measurements were taken at sub-zero
140 temperatures. When passing through dense liquid cloud, these sensors are known to underestimate temperature by up to a few degrees C due to wetting (Lawson and Cooper, 1990), so we use the out-of-cloud temperature at the same altitude to estimate cloud temperatures. In parts of the cloud that are not at their level of neutral buoyancy, the in-cloud temperatures may be up to a few degrees Celsius warmer or cooler due to the energies associated with changes in the phase of water molecules (Wang
145 and Geerts, 2009). A de-iced Aventech AIMMS-20 turbulence probe (Beswick et al., 2008) was used to measure the 3-D wind vector at 20 Hz. The stated accuracy of the AIMMS vertical wind (W) is $\sim 0.75 \text{ m s}^{-1}$, though intercomparisons between the AIMMS and the BAe-146's radome-mounted 5-port turbulence sensor agreed within around 0.5 m s^{-1} .

2.2.2 Cloud instrumentation

150 Cloud droplets with diameter $3 \leq D_P < 50 \mu\text{m}$ were measured using a Droplet Measurement Technologies (DMT) cloud droplet probe (CDP) (Lance, 2012). The CDP was calibrated several times during the campaign using glass beads (Rosenberg et al., 2012), and the sample area was measured to be 0.517 mm^2 using the droplet gun method (Lance et al., 2010). For more reliable sizing, bins 4 – 7 and 8 – 11 ($6.1 – 8.1 \mu\text{m}$ and $7.6 – 12.6 \mu\text{m}$ diameter) were combined to minimise the effect
155 of Mie sizing ambiguities, which caused systematic spikes in the size distributions. LWC was calculated by integrating the CDP size distribution and, on the flight discussed in this analysis, the values generated this way agreed with the onboard Johnson-Williams hotwire probe within $\sim 12\%$ below $\sim 0.9 \text{ g m}^{-3}$ (on the CDP), above which the hotwire probe began to saturate. The reported LWC values are from the CDP, as the hotwire probe suffered from wetting and saturation artefacts.

160 Larger cloud particles were measured using a Stratton Park Engineering Company (SPEC) 2DS stereo probe (Lawson et al., 2006) and a DMT cloud imaging probe-100 (CIP100, Baumgardner

et al., 2001), which are optical array probes (OAPs) that capture the size and shape of particles by measuring the shadow they cast on a photodiode array as they pass through a laser. The 2DS has a nominal size range of 10 – 1280 μm , with a resolution of 10 μm . The CIP100 captures larger particles 165 but in less detail, with a nominal size range 100 – 6400 μm and 100 μm resolution. All the OAPs were fitted with anti-shatter tips to reduce shattering artefacts (Korolev et al., 2011). A comparison of example size distributions measured by the three probes is presented in Fig. 1, which shows broad agreement between the probes where their size ranges overlap. The CDP, 2DS and CIP100 all use the measured true airspeed from the on-board 5-hole turbulence probe to calculate sample 170 volume. A comparison of the turbulence probe airspeed to that derived from the AIMMS probe showed both measurements were consistent within $\pm 2\%$. Since the AIMMS is located in a similar underwing location to the particle probes, this gives confidence in their calculated sample volumes. A description of the 2DS and CIP100-image analysis is provided in Appendix A. Additionally, we use the method described by Harris-Hobbs and Cooper (1987) to calculate the ice production rate (P_0) 175 in regions where columns comprise the majority of ice crystals. Further details of this calculation are given in Appendix A2.

Additional images of hydrometeors were obtained using a SPEC cloud particle imager (CPI, Connolly et al., 2007). Unlike the OAP probes which utilise 1-D detector arrays, the CPI utilises a 2-D CCD camera, which results in greatly enhanced image quality (8-bit greyscale images, 2.3 μm pixel 180 size). Quantitative hydrometeor concentrations could not be determined from the CPI during COPE, but the images collected provide further insight into the shape of the hydrometeors encountered. The CPI images shown in this manuscript have been processed by increasing the brightness by 40% and contrast by 20% to clarify the images.

2.2.3 Aerosol instrumentation

185 Total aerosol number concentration for sizes larger than 2.5 nm was measured using an Aerosol Dynamics Inc. model 3786-LP water-filled condensation particle counter (WCPC, Hering et al., 2005), based on the TSI model 3786 modified for use at low pressure. The aerosol size distribution was measured with a wing-mounted Particle Measurement Systems passive cavity aerosol spectrometer probe-100X (PCASP), with electronics upgraded by DMT, which was calibrated as detailed by 190 Rosenberg et al. (2012). The PCASP measures the dry optical size of particles 0.1 – 3 μm in diameter. Out of cloud, the CDP can also be used to detect aerosol >3 μm optical diameter, though this measurement is performed at ambient humidity, whereas the other probes use dried airflows.

Aerosol composition was sampled with an Aerodyne Research Inc. compact time-of-flight aerosol mass spectrometer (AMS, Drewnick et al., 2005; Canagaratna et al., 2007), which reports submicron 195 nonrefractory organic aerosol (OA), sulphate (SO_4^{2-}), nitrate (NO_3^-), ammonium (NH_4^+) and non-sea salt chloride (Cl^-_{NSS}). Refractory black carbon (BC) concentrations also measured using a DMT single-particle soot photometer (SP2 Stephens et al., 2003; Schwarz et al., 2010), with optics and

electronics upgraded to be functionally identical to the current SP2 model D. The SP2 was calibrated with Aquadag as recommended by (Baumgardner et al., 2012; Laborde et al., 2012). Further details
200 on the aerosol instrumentation and measurements will be provided in a future manuscript.

2.3 UWKA instrumentation

The UWKA measured cloud drops 2 – 50 µm in diameter using a DMT CDP calibrated by the manufacturer. Larger cloud particles were imaged using a DMT CIP-25GS (CIP25 hereafter) and Particle Measuring Systems 2DP probes, which are OAP probes with nominal diameters 25 – 1600 µm and
205 200 – 6400 µm respectively. Habit classification was performed on the CIP25 data, as described by Korolev and Sussman (2000). This analysis outputs the fraction of particles with >20 pixels that are classed as ‘spheres’, ‘irregulars’, ‘needles’ or ‘dendrites’. The 20-pixel threshold typically corresponds to a diameter of ∼ 125 µm for particles with an axial ratio of order 1.

The Wyoming Cloud radar (WCR, Wang et al., 2012) is a 95 GHz Doppler radar with beams
210 pointing vertically up and down (relative to the pitch and roll of the aircraft) and down-forward, though only the vertical data are discussed here. The along track (horizontal) and along beam (vertical) resolutions were approximately 6 m and 30 m respectively, for a nominal airspeed of 100 m s⁻¹ and 16 Hz sampling frequency. The WCR measured reflectivity and Doppler velocity, which is a convolution of particle fall speed and the vertical wind velocity. When precipitation-sized particles
215 are present they tend to dominate the reflectivity, leading to Doppler velocities considerably lower than the vertical air velocity. Data < 3 standard deviations of the measured noise were removed to clarify the images while having a minimal effect on the measured cloud data. Data were also removed when the UWKA was flying >10° from horizontal (i.e. the vertical radar beams were not pointing to the zenith and nadir). The UWKA was also fitted with downward-pointing lidar, described by Wang
220 et al. (2012), which was used to estimate cloud top height during overpasses.

2.4 NCAS precipitation radar

The ground-based NCAS mobile precipitation radar (Blyth et al., 2015) is a dual-polarisation 9.4 GHz Doppler radar with 2.4 m diameter antenna, resulting in a 1 ° beam width. During COPE the precipitation radar was located at Davidstow airfield (50.6369°N, −4.6106°E), which is near the centre of
225 the study area. When operating, the precipitation radar performed 360° plan position indicator (PPI) scans over a specified range of elevation angles. PPI scans were collected every 20 s. During the morning and early afternoon on 3rd August, barring a gap in sampling between 1158 – 1253 UTC, scans were performed at 1° intervals centred between 0.5° – 9.5° elevation. After 1436 UTC, the scan profile was changed to 0.5° – 18.5° elevation, at intervals of 2°, in order to ensure sampling of
230 the tops of the clouds. A series of scans across the full range of elevations took ∼ 4.5 min. The ability to obtain such a rapid sequence of multi-angle PPI scans meant that separate range-height indicator (RHI) scans of the clouds of interest were not required. The precipitation radar measured reflectivity,

radial velocity and dual-polarisation parameters including differential reflectivity, specific differential phase and copolar cross correlation coefficient, out to 150 km range with a resolution of 1° and
235 150 m in the azimuthal and radial directions respectively. We use the NCAS precipitation radar as an additional estimate of cloud top height, as well as to show the structure of cloud during the aircraft penetrations.

3 Results

3.1 Sampling overview

240 The meteorological conditions on 3rd August 2013 were typical of those described in Sect. 1. A low pressure system 300 km northwest of northern Scotland and a weak low over the mid-Atlantic brought moist air over the Southwest Peninsula from the southwest. A convergence line was forecast along the peninsula, and the only weather fronts over the UK were over northwest Scotland. [Figure 2 shows the vertical profile of wind speed and direction. The wind direction was southwesterly and](#)
245 [showed little variation with altitude. The wind speed was \$8 - 13 \text{ m s}^{-1}\$ up to 3 km, then increased with height to reach \$19 \text{ m s}^{-1}\$ by 5.8 km.](#)

Figure 3(a) shows the temperature and dew point from a radiosonde launched from Davidstow at 1500 UTC. There were also launches during the measurement period at 1200 UTC and 1345 UTC, however these probes both passed through cloud on their ascent. The air was moist throughout the
250 lower troposphere, with the RH staying above 70% up to a level of 3.5 km AMSL (hereafter, all altitudes are AMSL). Above this level the air became progressively drier with altitude, which would have limited clouds' ascent. There was also a weak inversion at around $\sim 5.3 \text{ km}$ ($T \sim -15^\circ\text{C}$), which appeared to cap the tops of the highest clouds.

Figures 3 (b) – (f) show the vertical profile of cloud measurements made by the BAe-146 during
255 the whole flight. Cloud base was at $\sim 1 \text{ km}$ ($T \sim 11^\circ\text{C}$), and the 0°C level was at $\sim 2.7 \text{ km}$. The maximum cloud drop number concentration measured by the CDP (N_{CDP}) was $\sim 400 \text{ cm}^{-3}$, which is not atypical for cumulus clouds, especially over land and where there are strong updrafts at cloud base. The maximum measured values of LWC approached those calculated in adiabatic parcels in the lower cloud passes, with the adiabatic fraction, f_{Ad} , up to 0.85. The reader should note, however,
260 that the values of f_{Ad} in the first few hundred metres above cloud base are particularly sensitive to the cloud base altitude used to calculate the adiabatic LWC. At higher levels, f_{Ad} generally decreased with altitude, probably due to a combination of precipitation scavenging, entrainment and conversion to ice.

The maximum number concentration of drops in the 2DS round category (N_{Round}) generally
265 increased with altitude, but the maximum concentrations of ice (N_{Ice}) and N_{CDP} were more variable. Ice concentrations of several hundred per litre were present in the H-M temperature range ($-3 > T > -8^\circ\text{C}$), but also at lower temperatures. Most of the penetrations within a few hundred

metres of cloud top were at temperatures between -10°C and -12°C , though some cloud tops reached temperatures as cold as -15°C , which corresponds to the temperature of the inversion at 270 5.3 km.

Figure 4(a) shows the estimated precipitation rate from the UK operational radar network (Met Office, 2003) at various points during the afternoon. Most of the clouds formed along two convergence lines running approximately southwest to northeast. Multiple cells (both isolated and interlinking) moved northeast along the lines. In Fig. 4 we define axes AB and CD along these two lines, in 275 order to provide reference points for the rest of our analysis. Some clouds deviated off the centre line of these axes, and in some sections, cells grew large enough to interact with those from the other line. Some sections were continuous lines of cloud, with multiple cells merging with those further up/downwind as they developed. Other sections contained isolated clouds, or adjacent cells interacting where their edges met.

280 Figure 4 (b) & (c) show the altitude of each aircraft and sampling focus at different stages of the flight. The UWKA operated at higher altitudes compared to the BAe-146, making penetrations through cloud tops and characterising cloud from above using its downward-pointing radar. The UWKA alternated between sampling lines AB and CD, making runs along and across the lines to investigate individual cells.

285 The BAe-146 initially performed low-level runs across and along the peninsula to characterise the boundary-layer aerosol. The average aerosol concentration and composition is summarised in Table 1. Around 80% of the accumulation-mode aerosol was ammonium sulphate, with smaller contributions from organic aerosol and ammonium nitrate. The small amounts of chloride detected are likely to be an underestimate, as the AMS is not able to detect sea salt. The total aerosol number concentration 290 was 6600 cm^{-3} . The composition and low total mass loading are indicative of fairly clean marine air, but the relatively high number concentration suggests new particle formation may have occurred on the flying day. The concentration of aerosol particles greater than $0.5 \mu\text{m}$ in diameter was 5 cm^{-3} . In Sect. 4 we use this concentration to estimate IN concentrations to within an order of magnitude using the parametrization of DeMott et al. (2010).

295 Following the low-level aerosol runs, the BAe-146 performed a series of straight and level runs along line AB at altitudes of 1.3 km ($T \sim 9^{\circ}\text{C}$) and 2.55 – 2.6 km ($T \sim 0^{\circ}\text{C}$). Several clouds were sampled near the southwest of the peninsula, with cloud tops generally below 3.5 km ($T \sim -5^{\circ}\text{C}$), containing $0.1 - 0.5 \text{ g m}^{-3}$ LWC and ice particle number concentrations $< 1 \text{ L}^{-1}$. As the focus of the flight was to study ice formation, the sampling shifted to line CD, where cloud tops grew to > 5 300 km. Passes were made by the BAe-146 at altitudes from 2.5 to 4.9 km ($0 < T < -12^{\circ}\text{C}$) and by the UWKA from 4.1 to 5.4 km ($-7 < T < -15^{\circ}\text{C}$).

The analysis in the following sections is divided up into three complementary parts, and a summary of the runs discussed is listed in Table 2. Firstly, we use in situ and radar measurements to characterise the phase, dynamics and spatial scales of a 40 km long semi-continuous section of

305 cloud along line CD. We then perform a similar analysis detailing the glaciation of a cloud that was initially physically separated from this line, but subsequently developed to merge with a section downwind as it glaciated. Finally, we present data from a penetration through the next cloud upwind, which showed evidence of the same microphysical processes occurring.

3.2 Characterisation of a line of closely-packed cells

310 Between 1325 and 1341 UTC, the BAe-146 flew three runs along a section of closely-packed cells along line CD, at temperatures between -5°C and -6°C . The clouds formed a quasi-stationary convective line with regenerating upwind convective cells. The ground-based precipitation radar observed newly-formed cloud regions increasing in height and reflectivity as they matured and moved downwind. The timescale from initiation, development of precipitation and dissipation was of the
315 order of one hour, though mixing between different cloud regions meant the precise age of any one region was often difficult to determine. The clouds were semi-continuous at the flying level, but had distinguishable tops. Figure 5 shows in situ microphysical data recorded during one of these runs, as well as images recorded by the 2DS in highlighted sections. The upwind (<35 km along axis CD) section of the line sampled tended to be mostly composed of liquid drops $<50\ \mu\text{m}$, whereas in the
320 section $35 - 60$ km along axis CD the cloud was mostly glaciated.

The effective radius (calculated from a combined size distribution using data from the CDP, 2DS and CIP100) The variable R_{32} in Fig. 5 is defined as the ratio of the third to the second moment of the hydrometeor size distribution generated by combining All-Accept data from the CDP, 2DS and CIP100. For spherical drops, this is the same as the effective radius; when used in clouds containing
325 nonspherical ice particles it is simply a useful indicator of the average particle size. R_{32} showed a general increase between $20 - 60$ km along axis CD, with the largest ice around $50 - 55$ km along axis CD. There was however a high degree of spatial inhomogeneity; the cloud phase and the concentrations and size of ice and liquid drops varied every $0.5 - 3$ km. Figure 4a shows that point C is close to the origin of the line of clouds, but new updraft cells also emerged further downwind.
330 Some are visible on Fig. 5 (e.g. at 30 km, 33 km and 56 km along axis CD), but new cells also developed to the northeast of point D.

Dynamically, the upwind section of the line sampled (<35 km along axis CD) was more active, with the strongest vertical motion in the liquid and mixed-phase parts. The more mature, glaciated stratiform regions were mostly quiescent. The spatial scale of the vertical motion was shorter than
335 that of the composition, varying every $50 - 500$ m, though some sections were consistent for a few kilometres. Blyth et al. (2005) also reported two length scales in small cumulus in Florida, one (around 1 km) associated with the width of the clouds and one ($200 - 500$ m) associated with the structure of the thermals. In Fig. 5, there is evidence from the vertical wind structure and concentration of cloud drops that several clouds had merged along the line.

340 In Fig. 5 we highlight five regions (marked by Roman numerals) to identify key processes occurring in the cloud at this level. These vary in phase, ice habit and dynamical structure. Regions I – III were parts of the line that had emerged 30 mins earlier, but was still active dynamically, with new cells emerging on the edges of pre-existing cloud regions. Regions IV and V were further downwind in a region that originated around an hour earlier, passed through a dynamically active phase but was
345 now quiescent and stratiform. The reader should consult Appendix A for details of the 2DS categories. Our constraint on cloud top temperature is limited in this case as it was above the maximum elevation of the precipitation radar for most of the run, but it is possible to provide an estimate that is likely to be accurate within a few degrees C.

Region I contained cloud which was composed almost entirely of liquid drops $<50\text{ }\mu\text{m}$. N_{CDP} was around 200 cm^{-3} . ~~The presence of both cloud droplets smaller than $13\text{ }\mu\text{m}$ and larger than $24\text{ }\mu\text{m}$ in diameter are thought to be a necessary condition of H-M (Mossop 1976, 1978). In Region I there were around 100 cm^{-3} of droplets smaller than $13\text{ }\mu\text{m}$ and 20 cm^{-3} larger than $24\text{ }\mu\text{m}$ in diameter, satisfying this condition.~~ The LWC was up to 1.47 g m^{-3} , and the effective radius was $\sim 14\text{ }\mu\text{m}$. The LWC was the highest that was measured on this run, meaning this region had undergone less
350 of the processes that deplete liquid water (entrainment, precipitation and ice formation) than other regions on this run. The BAe-146 passed through the centre of the cell, so reduced entrainment would be expected in this region compared to the regions downwind where the aircraft flew through the cloud edges. Dynamically, this region contained two updrafts up to 7 m s^{-1} separated by a thin downdraft of 4 m s^{-1} . The concentrations of particles measured by the 2DS that were large enough
355 to be classified by shape (N_{D90} , $>\sim 90\text{ }\mu\text{m}$) were $2 - 12\text{ L}^{-1}$ in total. Around half were classed as low irregularity (LI) meaning they were larger liquid drops, and the rest were rimed graupel. The graupel may have fallen from cloud top, which was likely within a few degrees of -11°C , or been brought down in the downdraft. In liquid clouds such as this, the cloud top height (and temperature) are likely to be an underestimate (overestimate), as the precipitation radar is unable to detect the low
360 reflectivities at the very top of the cloud. In contrast, almost no ice was measured in the pass through the young cell on the upwind end of Fig. 5 (around 15 km).

Region II was mixed-phase, with $\sim 0.5\text{ g m}^{-3}$ of liquid water and $39 - 78\text{ L}^{-1}$ of ice. Dynamically, the region was a mix of updrafts and downdrafts up to around $\pm 3\text{ m s}^{-1}$ which, combined with the presence of ice, suggest a more mature cloud than in Region I. The ice habits were a mix
370 of pristine columns, hollow columns and small to large graupel. ~~The ice concentrations and habits are a strong suggestion of the H-M process having taken place in this region. N_{CDP} was around 60 cm^{-3} , with 30 cm^{-3} smaller than $13\text{ }\mu\text{m}$ and 10 cm^{-3} larger than $24\text{ }\mu\text{m}$, meaning all the required conditions of H-M were met, and it is likely that H-M was still actively taking place.~~

Region III contained a cell with an updraft of $5 - 8\text{ m s}^{-1}$. The phase was similar to Region I in
375 that it was composed almost entirely of liquid drops, but N_{CDP} and the LWC were around one third of those in Region I. The BAe-146 passed through the northern edge of this cell, and did not penetrate

the region of highest radar reflectivity (not shown). The LWC and cloud drop concentration are likely to have been higher in the cell centre. N_{Round} was slightly higher than in Region I, up to 9 L^{-1} , and the graupel concentrations were around 5 L^{-1} . The NCAS precipitation radar data suggested the
380 cloud top was within a few degrees of -9°C . On the edges of Region III were downdrafts of $\sim 2 \text{ m s}^{-1}$ containing over 100 L^{-1} of columnar ice in downdrafts. These may represent more mature regions of this cloud, where H-M splinters ice particles had had time to grow to $>90 \mu\text{m}$ to be classified as ice by the 2DS.

Region IV contained mature, glaciated cloud with $90 - 270 \text{ L}^{-1}$ of ice and very few liquid drops.
385 The ice crystals were mostly pristine columns and hollow columns, with some graupel. The region was fairly quiescent, with a slight downdraft of up to 2 m s^{-1} . Further downwind, regions with similar phase but larger effective radius were composed of larger columns and aggregates. ~~The calculated rate of ice production in Region IV was $\sim 0.14 \text{ L}^{-1} \text{s}^{-1}$. The details of this calculation are given in Appendix A2. This value shows fairly good agreement with values from regions of secondary ice production reported by Harris Hobbs and Cooper (1987) and Huang et al. (2008).~~
390

Region V showed the top of a new updraft cell (or possibly multiple cells) penetrating through a pre-existing region of ice cloud containing $60 - 80 \text{ L}^{-1}$ of mature columns and aggregates. Regions of updraft up to 6 m s^{-1} were seen, containing LWC up to 0.5 g m^{-3} , and also ice with the same habits as the ice regions, although in lower concentrations of $10 - 50 \text{ L}^{-1}$. As in Region III, the BAe-
395 146 passed through the northern edge of these new cell(s), so the LWC and cloud drop concentrations were likely higher in the centre of the new updraft cell, where the radar reflectivity was higher. Following the aircraft penetration, these new updrafts developed into a reinvigorated dynamic cloud system. ~~The penetration through this region shows that new updraft cells further along the line may be seeded with ice from pre-existing clouds.~~

In summary, a run along the line of cloud at $T \sim -5^\circ\text{C}$ showed closely-packed cells, each at a different level of maturity and with different cloud drop and precipitation size, phase and dynamic structure. The upwind end of this section of the line contained mostly less developed clouds composed of liquid cloud drops, whereas further downwind the clouds were mostly glaciated, containing columns, aggregates and rimed graupel. The predominantly liquid clouds with tops colder than
400 $\sim -9^\circ\text{C}$ contained graupel in concentrations of a few per litre. New updrafts further downwind penetrating pre-existing regions of ice cloud contained mature ice, as would be expected if ice and precipitation particles were being recirculated into new updrafts. At this altitude and temperature level, the highest ice concentrations were associated with high concentrations of columnar crystals which are the preferred growth habit at near water saturation. ~~We infer from this that these high concentrations of columnar ice crystals must have spent most of their lifetime at or near this altitude, rather than being transported from above or below. As we have also identified that the conditions required for the H-M process (i.e. the presence of graupel as well as cloud droplets both smaller than $13 \mu\text{m}$ and larger than $24 \mu\text{m}$ in diameter) were present in weak updraft regions upwind (and up-shear) from~~
410

these high concentration regions, it is reasonable on the basis of previous observations (Blythe and Latham, 1993; Huang et al., 2008) to infer the action of the H-M process.

3.3 Glaciation within a confined cloud region

On the left (upwind) side of Fig. 5 is a newly-developing cloud, horizontally separated from the continuous line by ~ 5 km. Between 1330 – 1350, the BAe-146 made three passes through this turret at the southwest end of longitudinal runs along the line. It then made a further five runs, at increasing altitude, aiming specifically at this cloud, over a period of 20 min. Over a similar time period, the UWKA also made four passes over or penetrating the top of the cloud, the first and last of which are shown in Fig. 6. In total, this particular cloud was sampled over a period of ~ 40 min as it moved downwind, during which time multiple updraft thermals would be expected to develop and decay, each lasting 5 – 10 min (French et al., 1999).

3.3.1 Overpass and cloud top characterisation

For the overpass, shown in the left side of Fig. 6, the aircraft was ~ 1.5 km above cloud top, so the in situ probes did not measure any cloud particles. The value of the reflectivity was relatively low (generally below -5 dBZ), meaning that precipitation-sized particles can only have been present in small concentrations. For comparison, the peak reflectivity of -3 dBZ is equivalent to a concentration of 0.5 m^{-3} of 1 mm raindrops, 500 L^{-1} of $100 \mu\text{m}$ drops, or 2000 cm^{-3} of $25 \mu\text{m}$ drops. The vertical velocity data in Fig. 6d show the vertical motion of the hydrometeors, which is the net sum of the motion of the air parcel and the motion of particles falling gravitationally through it. Therefore in regions of upward vertical motion, the air is unambiguously moving upwards, whereas a net downward motion of particles may be due to downdraft and/or falling precipitation. Dynamically, the main turret was split in two, with an updraft region (up to 7 m s^{-1}) on the upwind side and downdraft section (up to 9 m s^{-1}) on the downwind side. Similar longitudinal runs sampled by the WCR, and cross-sections along the wind direction using the NCAS precipitation radar data showed that features in this line often had a similar diagonal structure, though not always such a clear divide between different dynamic regions. In this case, the low reflectivity suggests the cloud drops were relatively small, meaning the net downward motion is unlikely to be caused by precipitation. The vertical wind shear, with stronger winds aloft, meant the features had a diagonal divide rather than vertical.

During the run at 1356, the UWKA penetrated cloud top at an altitude of 4860 m ($T \sim -13^\circ\text{C}$). The value of reflectivity was higher than in the overpass that had occurred 25 minutes prior, meaning the average particle sizes had increased compared to the previous pass. Between 22.5 – 24.7 km along axis CD the WCR could not observe the lower sections of the cloud due to beam attenuation by the larger particles. There was still a clear region of falling particles downwind, which persisted down to ground level, and the updraft region was less continuous, which may be due to turbulent

motion or large precipitation falling through a more continuous updraft region. The in situ wind measured at cloud top showed several small pockets of updrafts of a few metres per second, and a 4 m s⁻¹ downdraft on the downwind side.

N_{CDP} at cloud top was 120 – 180 cm⁻³, and the concentration of particles larger than 125 µm (N_{D125}) measured by the CIP25 was $\sim 80 \text{ L}^{-1}$. Across the whole penetration, the habits classifications for particles >125 µm were 69% irregulars, 29% spheres and 2% needles, meaning there was $> 50 \text{ L}^{-1}$ of ice at cloud top. The droplet concentrations at cloud top were lower than those in young clouds in Fig. 5, but similar to some sections of mixed-phase cloud and penetrations near the edge of liquid turrets.

3.3.2 In situ characterisation

The BAe-146 made a series of runs through the developing cloud, increasing in altitude with time. The cloud composition and vertical velocity from these runs are shown in Fig. 7, and the maximum ice concentrations measured in updraft and downdraft regions, as well as the run/cloud top altitude/temperature and calculated IN concentrations, are listed in Table 2. The reported cloud top altitudes are the maximum within the turret, based on observations made by the UWKA radar/lidar and NCAS precipitation radar during the same time period. It is clear though in Fig. 6 that, within the main turret, cloud top varied by up to $\sim 800 \text{ m}$. The predicted IN concentrations are calculated using the DeMott et al. (2010) parametrisation, and are discussed further in Sect. 3.4. Figures 8 – 10 show images recorded by the 2DS and CPI during selected runs, and Fig. 11 shows the ground-based radar reflectivity to place each run into context, showing the horizontal cloud structure and the part of the cloud the aircraft passed through. For safety reasons, the BAe-146 avoided regions of highest reflectivity, meaning some of the passes were not through the centre of the turret. Consequently, in some of the cloud penetrations, particularly the later penetrations where the cloud was more developed and reflectivity was higher, the LWC and updraft strength may be biased low compared to the updraft cores.

As a general trend, in the earlier, lower altitude runs, the cloud was composed almost entirely of liquid cloud drops, and the peak LWC increased with altitude. This trend proceeded until significant precipitation was observed, at which point the LWC began to decrease, likely by scavenging and entrainment. At increasing altitude/time, the cloud shifted to mixed-phase and finally was nearly glaciated in the final run. Some variation in maturity of cloud regions, and concentrations within those regions, is to be expected due to penetrations through different parts of the cloud, but the general progression from young liquid cloud to mature ice cloud was still clear, as was the timescale over which this transition took place.

The first two runs in the turret (Runs 10.3 and 11.1) took place at temperatures of -3°C and -5°C respectively. The aircraft flew approximately parallel to the wind direction, and passed close to the cell centre in both penetrations. There were two main updrafts up to 4 – 5 m s⁻¹, with downdrafts

485 up to 2 m s^{-1} at the edges and in the centre. In Run 11.1, the downwind updraft region was more turbulent, with vertical velocity varying on the scale of tens of metres , where the upwind updraft
was 300 m wide . On both runs, the cloud was composed of up to $\sim 200 \text{ cm}^{-3}$ of cloud drops measured by the CDP, with LWC of $0.8 - 1.4 \text{ g m}^{-3}$. N_{D90} measured by the 2DS was $< 2 \text{ L}^{-1}$, and the measured particles were almost all round. Some of the 2DS images were classed as HI, but
490 it is difficult to tell if they were ice or just poorly-imaged drops. The high concentration of cloud drops meant the 2DS dead time fraction was high, and only a few D90 images were recorded, so the measured concentrations have a high counting error.

14 min later the BAe-146 made another run (Run 11.4) at the same altitude as Run 11.1, though in this time the cloud top had risen $\sim 900 \text{ m}$, and decreased in temperature from -6°C to -12°C .
495 The aircraft passed through two distinct regions- one containing updrafts $2 - 10 \text{ m s}^{-1}$ and the other downdrafts $0.5 - 7 \text{ m s}^{-1}$. The upwind side was a newer, younger updraft region developing on the side of the previous cell. The updraft side had higher LWC of $1.1 - 1.7 \text{ g m}^{-3}$, compared to $0.6 - 1.0 \text{ g m}^{-3}$ in the downdraft. N_{CDP} followed a similar trend, with $220 - 280 \text{ cm}^{-3}$ in the updraft and $120 - 170 \text{ cm}^{-3}$ in the downdraft. Although some 2DS data are missing in the updraft section due
500 to an instrument error, it is still clear from the remaining data that N_{D90} was significantly higher in the downdraft section, with N_{Round} of $5 - 60 \text{ L}^{-1}$ and N_{Ice} of $1 - 9 \text{ L}^{-1}$, compared to N_{Round} of $0.4 - 7 \text{ L}^{-1}$ and N_{Ice} of $0.4 - 3 \text{ L}^{-1}$ in the updraft. In the downdraft in Run 11.4, the ice particles were fairly circular in shape, suggesting they had originated as frozen drops. However, there is also some evidence of riming, and the smaller particles had a banding near the edge, which may suggest
505 a surface structure similar to the ridges often found on thin plates, though it is possible this banding is an optical/instrumental artefact. A few images of columns were also recorded. In the updraft, the images classed as HI were also fairly round, meaning they were either recently-frozen drops or simply poorly-imaged drops. The larger frozen drops were less rimed than in the downdraft, but some smaller particles also showed the banding present in the downdraft.

510 Run 13 took place four minutes after Run 11.4, and 300 m higher in altitude, but showed similar structure of an upwind side dominated by cloud drops in a strong updraft, and a downwind side with greater concentrations of particles large enough to be detected by the 2DS. The precipitation radar showed two distinct cells, and the aircraft passed close to the centre of both. The 2DS images in Run 13 were similar as those from the previous run, with a mix of drops, recently-frozen drops
515 and rimed round graupel. Compared to Run 11.4, the downwind side was more turbulent, and was predominantly updraft, whereas a similar region in Run 11.4 was predominantly downdraft. The LWC in the main updraft region reached 1.8 g m^{-3} , the highest that was detected in this developing cloud. N_{CDP} was also high here, at $170 - 270 \text{ cm}^{-3}$, but the highest droplet concentration was measured in the downwind side, where a small section of cloud contained N_{CDP} of 420 cm^{-3} in a
520 10 m s^{-1} updraft.

The next four runs were made at more oblique angles to the wind direction. By Run 14, the precipitation radar showed additional updraft cells/thermals had emerged on the downwind side. This cloud penetration showed several distinct sections; a central updraft of $1 - 8 \text{ m s}^{-1}$, close to the peak radar reflectivity, surrounded by dynamically mixed regions, and downdrafts on both the

525 upwind and downwind edges that were of similar strength to the updraft region. The peak LWC and N_{CDP} in the updraft region were 1.2 g m^{-3} and $\sim 180 \text{ cm}^{-3}$ respectively, which were around $1/3$ lower than in the previous run. N_{Ice} and N_{Round} in the updraft were higher than in the previous two runs, with N_{Ice} ranging $4 - 15 \text{ L}^{-1}$, and N_{Round} ranging $7 - 30 \text{ L}^{-1}$. The images in Fig. 8 show ice in the updraft was a mixture of small columns, **recently frozen drops and rimed ice.** The frozen

530 **drops had some riming but were still recognisable as frozen drops, so are likely to have frozen fairly recently.**

Compared to the updraft region, the 2DS measured enhanced concentrations in both downdrafts, with N_{Round} up to 90 L^{-1} and N_{Ice} up to 71 L^{-1} . These are far in excess of the concentrations seen lower down in the cloud. Although newly developing cells on the downwind side had begun to fill the

535 gap between the cloud region in question and cloud downwind, the highest ice concentrations in this run were sampled on the upwind side, meaning they cannot have been mixed in from a cloud further downwind. The images in the downdraft show large graupel and small irregular ice of indeterminate habit. The CPI images from Run 14 (Fig. 10) show pristine and rimed columns and heavily-rimed particles.

540 The BAe-146 passed through the same part of the cloud in the next run, Run 15.1, and measured a similar dynamical structure. Compared to the previous run, N_{Ice} and N_{Round} were enhanced in the central updraft region, ranging $19 - 78 \text{ L}^{-1}$ and $5 - 40 \text{ L}^{-1}$ respectively. N_{D90} decreased towards the centre of the updraft region, which suggests the larger particles had been mixed in and recirculated from more mature regions. The images in Figs. 8 and 9 show these were a mix of small

545 columns/hollow columns and small to large graupel. The LWC in the cloud drops was significantly lower than previous runs, peaking at 0.7 g m^{-3} , suggesting one, or some combination of all of the following: some of the small liquid drops had coalesced to form larger drops, some liquid water had changed to ice, and/or entrainment had diluted the cloud with dry air. Ice images in the downdraft were rimed small irregular ice, rimed columns and graupel, and two particles imaged by the CPI

550 had plate-like features, suggesting they had grown in part by vapour deposition at temperatures $< -10^\circ\text{C}$.

Run 15.2 was a transect across a more upwind section than Run 15.1, but showed similar ice habits. There was a clear divide between the younger updraft region dominated by cloud drops and the downdraft composed mainly of larger drops and ice.

555 Run 16 was the final run through this developing cloud region and, by this point, the gaps between it and the continuous line of cloud downwind had been filled. The section of cloud passed through on this run was largely quiescent. Although some small updrafts and downdrafts up to a few m s^{-1}

were present, the ice habits were very similar in these sections. The CDP measured almost zero, meaning all cloud drops had been lost by riming onto ice and/or evaporation. Some larger drops
560 were measured on the 2DS, but in smaller concentrations than the previous few runs. The 2DS measured ice concentrations up to 205 L^{-1} , and these were generally heavily rimed, with elongated or round shapes suggesting they originated as columns or droplets.

3.3.3 Ice in the ~~following~~ turret next cloud upwind

After the runs shown in Figs. 7 – 11, the BAe-146 made three runs near the top of the ~~following~~ next
565 cloud to the southwest ~~upwind~~ along line CD (i.e. upwind), which took place as the cloud moved between 23 and 32 km along line CD. These runs were made at the same altitude as Run 16, and were on an axis of approximately $5/185^\circ$, along which the cloud was $\sim 5 \text{ km}$ wide. Data and images from the third of these runs, Run 17.3, are shown in Fig. 12. There were three distinct regions in
570 which the microphysical data were consistently different to each other, which are labelled I – III in Fig. 12.

Region I contained strong updrafts of up to 10 m s^{-1} , and the cloud in this region was mostly composed of liquid drops $< 50 \mu\text{m}$, with N_{CDP} up to 120 cm^{-3} . Drizzle-sized drops (i.e. those classed as ‘round’ by the 2DS) were present at concentrations of $30 – 65 \text{ L}^{-1}$, and ice in concentrations of $5 – 60 \text{ L}^{-1}$, most of which were heavily rimed graupel, with a few hollow columns. The
575 concentrations measured by the CDP, 2DS and CIP100 all decreased towards the downdraft section at the edge of the cloud, as did the effective radius. This reduction is likely to be due to entrainment of dry air into the cloud, as well as adiabatic evaporation in the downdraft.

Region II also had updrafts of up to 6 m s^{-1} but was mixed-phase, with $N_{Ice} > 170 \text{ L}^{-1}$. These were mostly columns or hollow columns, meaning they had originated ~~in the H-M zone at temperatures between around $-3 – -10$~~ , where columns are the dominant mode of depositional growth. The
580 CPI images show evidence of aggregation and some riming, but the columnar structure is still clearly visible. ~~The calculated ice production rate to sustain such an ice population was $0.11 \text{ L}^{-1} \text{ s}^{-1}$, which is consistent with that calculated in the H-M zone.~~ Compared to those in Region I the ice particles were larger, and the LWC of the cloud drops was much lower. This was likely due to riming and
585 conversion to ice via the Bergeron-Findeisen process, which may have occurred lower down in the cloud.

Region III represents a mature stage of the cloud, similar to that observed in Run 16, and contained the largest particles in this cloud. This region was mostly in a weak downdraft of up to 2 m s^{-1} , and the cloud drops had been entirely depleted, leaving only ice and some larger round drops left. The
590 ice was heavily-rimed, and displayed a mixture of plate-like and columnar features. ~~Though it is less clear that these ice particles were produced by H-M, aggregation and transport to different growth regimes can change the habit of ice crystals as they age. No laboratory-confirmed mechanisms of ice multiplication other than H-M process can explain the presence of these particles in such high~~

595 eonecentrations. It is possible that fragmentation of freezing droplets may have enhanced the ice concentrations, particularly higher up in the cloud where the warm rain process had produced larger drops. However, as we discuss in the next section, this is unlikely to be the main source of the high ice concentrations.

3.4 Summary of ice measurements

3.4.1 The formation of first ice

600 Section 3.3 described the glaciation of a cloud as it developed from an isolated young cloud into a mature region of the semi-continuous line. Several possible ice-forming processes may take place in a developing cloud. Primary ice may form as drops freeze by immersion nucleation, or by contact nucleation with interstitial IN. Primary nucleation is expected to form ice in concentrations within an order of magnitude of the IN concentrations calculated using the DeMott et al. (2010) parametrisation. Clouds forming under or adjacent to existing mixed-phase or ice clouds may be seeded with existing ice, which would accelerate their development. Figure 5 shows some evidence for ice seeding occurring in clouds further downwind, but Fig. 11 shows that the cloud region that was the focus of this analysis was initially isolated from neighbouring clouds by several kilometres, and no aerosol layers or regions containing outflow from previous clouds were detected in the immediate vicinity.

610 Even in the early stages of a cloud, some secondary ice processes may enhance ice concentrations. Primary ice undergoing riming in the H–M temperature zone may emit ice splinters, and larger drops may fragment into several pieces upon freezing. Rangno (2008) showed that this drop-freezing secondary ice production process can result in modest enhancements of $\sim 5\%$, though Lawson et al (2015) showed in tropical cumulus it can increase ice concentrations up to several hundred per litre.

615 Figure 13 provides a comparison of the mean ice concentrations in updraft and downdraft regions in the cloud and the predicted IN concentration calculated using the DeMott et al. (2010) parametrisation, which is based on the concentration of aerosols in the boundary layer exceeding a threshold diameter of $0.5 \mu\text{m}$. The aerosol concentration used in these calculations was taken from Table 1. The data from Fig. 13 are also summarised in Table 2. The DeMott et al. (2010) calculations have 620 an uncertainty of around a factor of 10, as they do not consider aerosol composition. Cloud top temperature was used in the calculation to provide an estimate of the upper limit of IN concentrations, as primary ice cannot form at cooler temperatures than the coldest temperatures in the cloud. Ice forming at cloud top may be transported to other regions in the cloud by precipitation and/or thermal recirculation, but would take time to descend to the measurement level.

625 No ice particles were measured during the run with cloud top at -4°C , and only a few were recorded on Run 11.1, when cloud top temperature was -6°C . The counting errors are large due to the poor sampling statistics, and the absolute concentrations may be biased high due to misclassified liquid particles. The mean ice concentrations were a factor of 5 – 15 higher than the calculated IN

concentrations, which is at the upper end of what might be expected from primary ice nucleation,
630 but it is difficult to make a quantitative comparison due to the large measurement uncertainty.

The next run was made at the same measurement altitude, but around 14.5 minutes later. In this time, the cloud top temperature had reached -12°C . The ice concentrations measured at -5°C had increased by around order of magnitude, but so had the calculated IN concentrations at cloud top. The measured ice concentrations were statistically significant, and 0.7 – 3 times the calculated IN
635 concentrations. Again though, poorly imaged drops may mean the ice concentrations in this run are overestimated.

The larger ice concentrations in the downdraft may suggest primary ice nucleation occurring at lower temperatures nearer cloud top. If the first ice formed predominantly from freezing small cloud drops or interstitial IN, rather than freezing drizzle, these particles would then have to grow by
640 vapour deposition to sizes $\sim 90 \mu\text{m}$ in order to be classed as ice by the 2DS. We would therefore expect to observe a larger fraction of the first ice as columns or plates, depending on the temperature at which the growth occurred. In fact, almost all the first ice images observed were frozen drizzle-sized drops, with variable amounts of riming. It is difficult to be definitively clear, but the evidence appears more consistent with the majority of the first ice forming as freezing drizzle.

645 The in situ observations during Run 13 were similar to those in Run 11.4, but with lower ice concentrations in the downdraft, and no columns were observed. The precipitation radar reflectivity in Fig. 11 shows two maxima at 3.5 km altitude, suggesting a second thermal was emerging, but at this stage any ice multiplication in updraft regions cannot have progressed to a stage where high ice concentrations had reached the downdrafts.

650 ~~The efficiency of the drop-freezing secondary ice production process is strongly linked to the concentration of drizzle- and rain-sized drops, as larger drops undergo greater fragmentation upon freezing (Lawson et al. 2015). The cloud base in this case study was $\sim 11^{\circ}\text{C}$ colder than those considered by Lawson et al. (2015), meaning the warm rain process had less depth of cloud to generate large drops before reaching freezing temperatures. The cloud drop number concentration here was also several times higher than those measured by Lawson et al. (2015). Consequently, the concentrations of larger drops entering ice-forming temperatures were much lower in this case, and the drop-freezing secondary ice mechanism would be expected to have much less of an effect.~~

660 ~~Lawson et al. (2015) stated that the presence of drops larger than $200 \mu\text{m}$ in updrafts at -6°C was required for significant ice enhancements by droplet fragmentation. The mean concentrations of $N_{\text{round}} > 200 \mu\text{m}$ in updrafts in runs 11.1, 11.4 and 13 were 0, 3.6 and 0.9 L^{-1} respectively. The average number of fragments expected from a $200 \mu\text{m}$ drop is 0.04 (Lawson et al. 2015, Fig. 12), meaning if all these drops were to freeze in the H-M zone only a minimal enhancement 4% would be expected.~~

665 The ice concentrations measured in the first few runs were mostly nearer the upper end of what might be expected from primary nucleation, so it is possible that the ice concentrations in the early

stages were enhanced by some secondary ice this mechanism. The droplet size distribution would also have been larger higher up in the cloud. It is clear, however, that there was no prolific secondary ice production in these early stages.

3.4.2 The transition to secondary ice

- 670 As cloud top reached -14°C , columns and rimed graupel were observed in updraft regions at -9°C by the BAe-146, as well as at cloud top by the UWKA. The images from the updraft in Run 14 look similar to those in the downdraft in Run 11.4, meaning the particles may have been recirculated from a previous downdraft. By this stage, new updraft cells had emerged on the downwind side, which brought a new supply of liquid water to mix with downdraft and quiescent regions , and provides a
675 mechanism to redistribute particles throughout the cloud. Not only does this provide a mechanism to redistribute particles throughout the cloud, secondary ice production is thought to be most prolific when new thermals emerge to bring a supply of liquid drops to the H-M zone (Blythe and Latham, 1987).

Run 14 was the first run where the measured ice concentrations showed a clear enhancement
680 compared to the calculated IN values. N_{Ice} measured in earlier runs were roughly within a factor of 10 of the calculated IN values, but in Run 14 and subsequent runs they were >30 times the calculated IN concentrations, and this enhancement increased with time. In order to generate such high ice concentrations, one or more secondary ice processes must have been active during these runs. We note that the highest ice concentrations measured during Run 14 were measured closer to
685 the upwind side (though the run was at a tangent to the wind axis), meaning ice seeding from pre-existing cells downwind cannot have been the source of the increased ice concentrations. The most likely explanation is that these were ice splinters that were lifted in the updraft regions, but had only grown large enough to be classified as ice by the 2DS once they had reached the downdraft regions.

In the later runs at higher altitude, the cloud top reached its lowest temperature of -15°C . The
690 process of recirculation continued, as columns, rimed graupel and frozen drops were found in the updraft in Run 15.1. This was the first time rimed columns were observed in the cloud, around 13 minutes after rimed frozen drops were observed in Run 11.4. As the cloud grew older and the cloud top reached lower temperatures, ice in the downdraft became more rimed, which suggests it may have been recirculated more than once, and the ice habits in the downdraft became more difficult to
695 distinguish. Some images had the appearance of rimed columns, and some of rimed frozen drops. The mix of columnar and plate-like features suggests growth by vapour deposition at temperatures with different dominant ice habits, though most of the growth in the larger ice crystals appears to have taken place by riming and aggregation. The crystal habits and ice concentrations of hundreds per litre make it clear that these particles were generated by the H-M process, and were lifted further
700 up in the cloud by updrafts.

In the mature stages, the cloud drops had been depleted through entrainment and conversion to ice, and the largest drops were fewer in number in Run 16 than mature regions in the preceding

few runs. Smaller droplets would have been lost by riming and all sizes of drop would shrink due to entrainment-induced evaporation. In the mature regions sampled lower down in the cloud on
705 Run 11.2, very few large drops were measured. These regions were generally fully glaciated, and contained only mature columns, aggregates and graupel, though the largest graupel had precipitated out.

Run 17.3 showed the same processes were occurring in the next cloud upwind. The images in Fig. 12 are the clearest, showing the mixed-habit, rimed ice particles. Region I in Fig. 12 appeared to
710 be a relatively young updraft composed mostly of cloud drops, with some large drops and ice. The concentrations of large drops and ice increased closer to the adjacent parts of the cloud containing more ice, as did the effective radius and concentration of large particles measured by the CIP100. Also, the ice particles that were measured in this region were rimed graupel and columns, rather than
715 recently-frozen drops that were present in earlier young updrafts. The concentration gradient and ice habits suggest that the ice particles in this updraft were recirculated, and that young cells emerging next to more mature ones are seeded with ice to hasten their development.

4 Discussion

4.1 Comparison to August 2004 case

The clouds in the 2004 Boscastle floods, and in the case presented in this manuscript, both formed
720 along convergence lines over the Southwest Peninsula of the UK. In both cases, the convergence lines were aligned with the peninsula in predominantly southwesterly winds (Golding et al., 2005). In the August 2004 case, a single line of cloud remained quasi-stationary near the north coast of the Southwest Peninsula for a period of 4 h. In our case, there were two lines of convective clouds, and they were both located further inland over the peninsula. The clouds were not as deep as those
725 present in August 2004, probably due to the dry air in the mid- to upper-troposphere and weak inversion at ~ 5 km that capped cloud tops. The maximum radar-estimated rainfall intensity for the clouds studied in this paper was $\sim 50 \text{ mm hr}^{-1}$, which is comparable to the maximum rainfall rate seen throughout much of the afternoon in August 2004, though less than the peak. The winds were stronger in this case, meaning the local duration of maximum precipitation from any individual cell
730 was reduced by comparison to the August 2004 case. The lines in this study only persisted for around 2 h, and no significant flooding was reported.

4.2 Horizontal development

During similar meteorological conditions, consecutive cumulus cells can often tend to initiate from similar locations (Bennett et al., 2006). The cloud sampled by the BAe-146 in Figs. 7 – 11 was
735 initially isolated, but grew horizontally to join the semi-continuous section of cloud downwind. Figures 4 and 5 show that the cloud tended to form semi-continuous lines of closely-packed cells

along the wind direction. The last few runs in Fig. 11 also show a subsequent cloud further upwind, which was initiated from a similar location, undergoing similar behaviour, and this is the cloud sampled in Fig. 12.

740 During runs 10.3 – 11.4 the cloud sampled had a reasonably similar dynamical structure. On the upwind side, the strongest updraft contained many liquid cloud drops and few large drops or ice. The strongest downdrafts tended to be located on the downwind side, though this region was also turbulent, and contained larger drops/ice meaning it was more mature than the updraft. The vertical velocity data in Fig. 6 (d) also show a diagonal structure- the boundary between updraft and downdraft sections was further downwind at higher altitude. Features exhibited similar diagonal structure in other longitudinal runs sampled by the WCR and precipitation radar, though the example shown in Fig. 6 is the clearest example of segregated updraft and downdraft regions.

745 This structure is a result of the unidirectional vertical wind shear in the region where the cloud developed , shown in Fig. 2 . Between the altitudes of the lowest and highest runs shown in Fig. 7, the average out-of-cloud vertical wind gradient was $\sim 3 \text{ m s}^{-1} \text{ km}^{-1}$. This would cause a relative motion in the upwind direction (i.e. towards point C) at lower altitudes, and in the downwind direction (towards point D) at higher levels. This dynamic setup elongates the cloud and its precipitation footprint horizontally, and aids recirculation by encouraging individual cells into this overturning structure.

750 755 Figure 9 shows the emergence of new updraft cells along the wind axis, incorporating the initially-isolated cloud region into a continuous line. Similar behaviour was observed by Golding (2005) in the August 2004 case. The wind shear extends individual cells horizontally, and facilitates recirculation by mixing in adjacent thermals.

4.3 Ice development

760 4.3.1 Generation of columns and mixed-habit ice crystals

The observations described in Sect. 3 demonstrated several key features which provide insight into the ice formation processes occurring in the clouds. Ice concentrations of up to several hundred per litre were observed in multiple cloud regions; firstly, in developing and mature cloud at $T \sim -5^\circ\text{C}$, and secondly at increasing altitude (decreasing temperature) in a single developing cloud region as 765 it matured. At $T \sim -5^\circ\text{C}$ the ice were mostly a mixture of frozen drops and graupel in developing clouds, and columns in more mature regions. At $T \sim -10$ to -12°C , the ice were a mixture of frozen drops, graupel and mixed-habit ice showing columnar and plate-like features.

770 The habit of vapour-grown ice crystals is determined by the temperature at which they undergo growth. Ice crystals growing in the range $-3 > T > -10^\circ\text{C}$ develop columnar features, whereas crystals growing at temperatures $T < -10^\circ\text{C}$ develop plate-like features. This provides us with some information on the history of such ice crystals. The pristine columns and aggregates of columns

measured in quiescent regions at $T \sim -5^\circ\text{C}$ during Run 11.2 must have formed and spent their entire lifetime at temperatures $-3 > T > -10^\circ\text{C}$. Alternatively, the near-pristine columns measured at temperatures $T = -10^\circ\text{C}$ in updrafts on Run 15.1 and $T = -12^\circ\text{C}$ in updrafts on Run 17.3 must
775 have grown (and almost certainly formed) at temperatures $-3 > T > -10^\circ\text{C}$ before being rapidly transported upwards. The mixed-habit columnar/plate-like ice crystals detected in quiescent regions at $T = -12^\circ\text{C}$ on runs 16 and 17.3 must have had a similar history before undergoing further growth at $T = -12^\circ\text{C}$ to develop plate-like features, while also undergoing riming.

We may gain further evidence that the columns detected at $T \sim -12^\circ\text{C}$ were generated by the
780 same mechanism as those detected at $T \sim -5^\circ\text{C}$ during Run 11.2. Using the method of Harris-Hobbs and Cooper (1987), as described in Appendix A2, the calculated rate of ice production in Region IV on Run 11.2 (a mature region containing columns), was $0.14 \text{ L}^{-1} \text{ s}^{-1}$. Using the same method in Region II on Run 17.3, a mixed-phase updraft region at $T = -12^\circ\text{C}$ containing predominantly columns, gives a calculated ice production rate of $0.11 \text{ L}^{-1} \text{ s}^{-1}$. The consistency of these
785 numbers provides further evidence that both sets of columns were produced by the same mechanism.

To summarise, it is clear that one or more secondary ice processes were active at temperatures $-3 > T > -10^\circ\text{C}$ and generated ice columns in concentrations of up to several hundred per litre. Some of these columns remained at similar temperatures, while others were lifted to higher levels in
790 updrafts.

4.3.2 Generation of frozen drops

Although columns were the dominant ice habit in many of the mature stratiform-stage clouds measured, a large fraction of the ice particles detected were frozen drops, particularly in the mixed-phase developing stages. It is more difficult to determine the temperature at which such particles froze as
795 they generally do not exhibit clear features of growth by vapour deposition. The time since these particles froze may be qualitatively estimated (i.e. recently-frozen or not) by the degree of riming around the edges. Frozen drops with minimal riming must have frozen at or near the temperature at which they were measured, whereas more heavily rimed graupel is more likely to have frozen at lower temperatures when found in downdrafts, or higher temperatures when found in updrafts.
800 The presence of frozen drops does not inherently reveal the origins of the ice; something must cause a drop to freeze, whether this is immersion or contact freezing with primary IN, or freezing when coming into contact with a pre-existing ice crystal. The concentrations of frozen drops were well in excess of the expected IN concentrations, so it is likely that one or more secondary ice processes were involved in freezing the drops.

805 Figures 7 and 13 show that ice concentrations were generally higher in or near downdrafts than in updrafts. Run 15.2 on Fig. 7 is a particularly clear example. It is also clear that while N_{Ice} was higher in these downdrafts, N_{Round} was also higher compared to updrafts. For much of the cloud's

development, updraft regions contained greater concentrations of small liquid drops, while down-draft regions contained higher concentrations of larger hydrometeors, some of which were drizzle, 810 and some of which were ice. The downdraft regions were, therefore, simply more mature regions of the cloud than the younger updraft regions. In order to have been detected in such downdrafts, the water contained in the drizzle drops must have travelled upwards in an updraft and grown into larger drops by collision-coalescence and condensation of water vapour, before reaching the downdraft. At some point along this trajectory, some fraction of the drizzle drops froze, and where this was due to 815 interaction with a secondary-ice forming process, they must have come into contact with pre-existing ice crystals.

The frozen drops in the downdrafts appeared more rimed and aged (i.e. less round) than those found in the updrafts. This means the frozen drops in the downdrafts were generally older, and are therefore more likely to have frozen nearer to cloud top. However, some recently-frozen drops were 820 recorded in runs 11.4 – 15.2, at measurements temperatures between -5 and -10 °C. The minimal amounts of riming on these particles means they must have frozen near the measurement level. The location at which the drops froze does not necessarily reveal the location at which the ice was produced. For example, a secondary ice splinter formed at -6 °C may be too small to observe in updrafts, but could have frozen a drizzle drop by the time it reached the same level in a downdraft. 825 Conversely, if the splinter was formed near cloud top, it may travel in a downdraft (possibly in subsaturated conditions) to freeze a drop at the measurement level.

Perhaps the clearest consistent trend in the developing cloud measured in runs 10.3 – 16 was that drizzle and ice were generally well correlated with each other, but anti-correlated with cloud drops. In these developing mixed-phase regions of intermediate maturity (i.e. not young, but not 830 yet glaciated), the development of ice and drizzle appeared to progress in parallel. Whatever ice multiplication processes were active, the majority of the early secondary ice went on to freeze drizzle drops, which formed the first large ice and precipitation-sized particles. Furthermore, regardless of the ice production mechanism, the freezing of drizzle drops accelerates the growth of large ice by being large when they freeze, providing a shortcut through the growth phase.

835 4.3.3 Secondary ice mechanisms

There are several known secondary ice production mechanisms, each with different required conditions. H-M is the most widely-acknowledged, and the best quantified, but requires specific conditions to be met. An alternative mechanism to gain recent attention is ice multiplication as supercooled drops freeze, either by fragmentation or spicule formation due to internal pressure. A third possible 840 mechanism is the fragmentation of pre-existing ice particles by ice-ice collisions.

H-M is active in the temperature range $-3 > T > -8$ °C, and requires the presence of graupel and cloud drops both smaller than 13 µm and larger than 24 µm in diameter (Mossop, 1976, 1978). Figure 1 shows a typical size distribution from a developing cloud at $T = -5$ °C, measured during

Run 11.2. This cloud drop size distribution was typical of liquid cloud sampled at this temperature.
845 In non-glaciated cloud regions on Run 11.2, droplets smaller than 13 μm and larger than 24 μm
were ubiquitous, and this was also true during runs in the developing cloud discussed in Sect. 3.3. In
terms of concentrations, in Region I on Run 11.2 there were around 100 cm^{-3} of droplets smaller
than 13 μm and 20 cm^{-3} larger than 24 μm as measured by the CDP. Graupel was also found in
all mixed-phase regions on Run 11.2 and, once ice formation had begun, in the developing cloud
850 discussed in Sect. 3.3. It is also clear, based on the images of graupel with different levels of riming,
that riming was actively occurring during our observations.

The expected products of H-M are large concentrations of columnar ice crystals, particularly
in the temperature range $-3 > T > -8 \text{ }^{\circ}\text{C}$, but also at other temperatures when transported by
up/downdrafts. Pristine or near-pristine columns were observed in concentrations up to several hun-
855 dred per litre, both in mature cloud in runs at $T = -5 \text{ }^{\circ}\text{C}$ and in updrafts at lower temperatures. In
mature regions at $T = -12 \text{ }^{\circ}\text{C}$, mixed-habit ice were found that must have spent part of their lives
growing as columns, before moving to temperatures where plates are the ice crystal growth regime.
Given that all the known conditions of H-M were met in developing clouds, and the expected prod-
ucts of H-M were found in mature clouds, it is very likely that H-M was operating.

860 Ice multiplication by freezing of supercooled drops has been postulated by several previous studies (e.g. Rangno and Hobbs, 2001; Rangno, 2008), but thusfar quantification has been very limited.
Possible mechanisms include shattering of drops into fragments, and the formation of spicules which
eject gas bubble membranes that break off into ice fragments. Both processes may produce micro-
scopic shards of ice, as well as large pieces that are recognisable as fragments of the shape of the
865 original drop that froze. Most previous studies with observations of shattered drops have estimated
droplet shattering may enhance ice concentrations by a modest amount (typically up to single-figure
percentages) (Korolev et al., 2004; Rangno, 2008), though Lawson et al. (2015) recently presented
some evidence that the process may enhance ice concentrations by multiple orders of magnitude
over a timescale of minutes in tropical cumulus. Lawson et al. (2015) showed images of fragments
870 of drops (i.e. frozen parts of the original spherical drop), and drops with protrusions that may be
partway through spicule formation.

In our observations, we did not observe any drops that were obviously partway through spicule
formation, and only two images of shattered drop fragments out of the thousand of images recorded
by the 2DS and CPI. We note, however, that in mixed-phase clouds the detection efficiency of the
875 CPI was poor, and many of the ice shapes recorded by the 2DS were somewhat irregular, making it
difficult to determine their origin and history. Many of the frozen drops recorded by the 2DS were
heavily rimed, meaning it is difficult to determine if any fragments may have broken off during
freezing. The efficiency of the drop-freezing secondary ice production process is strongly linked
to the concentration of drizzle- and rain-sized drops, as larger drops undergo greater fragmentation
880 upon freezing Lawson et al. (2015). The cloud base in this case study was $\sim 11 \text{ }^{\circ}\text{C}$ colder than

those considered by Lawson et al. (2015), meaning the warm rain process had less depth of cloud to generate large drops before reaching freezing temperatures. The cloud drop number concentration here was also several times higher than those measured by Lawson et al. (2015). Consequently, the concentrations of larger drops entering ice-forming temperatures were much lower in this case, and
885 the drop-freezing secondary ice mechanism would be expected to have less of an effect.

Modelling work by Lawson et al. (2015) suggested that the concentration of drops larger than 200 μm in updrafts at -6°C was an indicator for whether significant ice enhancements by droplet fragmentation would occur. The mean concentrations of $N_{\text{Round}} > 200 \mu\text{m}$ in updrafts in runs 11.1, 11.4 and 13 were 0, 3.6 and 0.9 L^{-1} respectively. Based on our observations alone we are not able to
890 quantitatively assess the potential of droplet freezing secondary ice formation to affect ice concentrations, but these numbers will serve as a reference point for microphysical simulations which are beyond the scope of this paper. Using our observations of frozen drops and a comparison between our droplet size distributions and the observations and modelling work by Lawson et al. (2015), we are able to say that secondary ice formation associated with droplet freezing is likely to have been
895 active in our case study, but to a lesser extent than in the tropical chimney clouds described by Lawson et al. (2015). The cooler cloud base in our case study means the drops were generally smaller when reaching freezing temperatures, and therefore less efficient at secondary ice production when freezing.

Fragmentation of ice during ice-ice collisions may be an additional secondary production mechanism.
900 Yano and Phillips (2011) studied this process using a highly-simplified conceptual model, and suggested it may rival H-M if sufficient concentrations of large supercooled drops were present to accelerate the formation of large graupel. The required conditions were the presence of millimetre-sized graupel, supercooled liquid and pre-existing ice crystals, which were all present in our case study once ice formation had begun. However, the presence of large supercooled drops and graupel
905 would also accelerate H-M (Phillips et al., 2001). Furthermore, the ice fragmentation rate used by Yano and Phillips (2011) was derived from laboratory studies using centimetre-sized balls of ice; other experiments using more realistically-sized graupel have found that the collision velocity required is much larger than would be found in the atmosphere (Griggs and Choularton, 1986). Again, it is difficult to quantify what influence this process may have had on our case study, but given the
910 lack of laboratory experiments confirming this process may occur in realistic conditions, it appears doubtful that it can have had a major influence on ice concentrations.

It seems most likely that the observed ice concentrations and habits described in Sect. 3 may be explained by a combination of H-M and droplet-freezing multiplication, though the relative importance of each process is not clear, and will depend on time and location within the cloud. Both of
915 these mechanisms may generate small ice fragments, which collide with and freeze larger drops due to their different fall speeds. Based on our observations, this appears to be the main pathway for production of precipitation-sized particles in the clouds, particularly in the intermediate stages of de-

velopment. In contrast, much of the ice in the mature, glaciated regions was in the form of columns or mixed-habit ice, which had undergone significant growth by vapour deposition. We suggest these
920 are likely to be small ice crystals that did not impact upon large drops and grew more slowly, so were left remaining once the frozen drops had precipitated out. The presence of columnar features in ice crystals in all the glaciated outflow regions suggests these particles were formed by H-M.

It is clear that both H-M and the droplet-freezing secondary ice mechanisms are intimately linked with the warm rain process. H-M requires specific sizes of cloud drops and may be accelerated by
925 graupel formed by frozen drops, and droplet-freezing multiplication is thought to be more prevalent when larger drops freeze. The temperature at which large concentrations of drizzle and raindrops form depends on the cloud base temperature, cloud drop number concentration and time-dependent factors such as updraft speed and cell lifetime. Conversely, the temperatures of the 0°C level and H-M zone are clearly fixed. In an atmosphere with a warmer cloud base, the concentrations of large
930 drops entering and exiting the H-M zone in updrafts and downdrafts would be higher, as would the fragmentation by the freezing of larger droplets. Conversely, a cooler cloud base would decrease the concentration of the larger drops. The warm rain process, and its interaction with secondary ice processes, appears key to determining the timing and location of precipitation.

5 Conclusions

935 We have outlined the microphysical mechanisms that resulted in the development of precipitation and the glaciation of a line of cumulus that formed along England's Southwest Peninsula. The line formed in the early afternoon on a convergence line along the peninsula, and was similar to a quasi-stationary band of cloud that caused severe flooding to the village of Boscastle in August 2004. The line of clouds became longer and broader during the afternoon as a result of the combination of
940 new cell formation and stratiform regions forming downwind of the convective cells. The glaciation process occurred in several stages:

- Primary ice nucleation formed the first ice particles in the initial cell. In agreement with Huang et al. (2008), the first ice and precipitation observed were frozen drizzle drops, rather than smaller ice grown by vapour deposition. The evidence therefore suggests that it was predominantly the larger drops that froze, rather than smaller, though this is not definitively clear.
945
- The concentration of ice particles increased slightly, either due to secondary ice formation occurring in the same thermal in which the supercooled raindrops froze, or increased primary ice nucleation as cloud top ascended, but significant enhancement of the ice crystal concentration was not observed until subsequent thermals ascended through the measurement H-M region.
- Increasing ice concentrations well in excess of that expected from primary ice nucleation signalled the onset of secondary ice production, and the necessary conditions for both H-M
950

and droplet-freezing secondary ice processes were met. The majority of the initial secondary ice particles were observed as frozen drops. Small ice caused drizzle drops to freeze on contact, forming additional instant-rimers. Larger drizzle and raindrops were preferentially frozen, as they were more likely to encounter splinters as a result of their larger size and fall speed.

- 955
- The recirculated ice initiated the H-M process, and this appeared to coincide with the development of new updraft thermals in the cloud. The ice production rates calculated using the method of Harris-Hobbs and Cooper (1987) were $\sim 0.1 \text{ L}^{-1} \text{ s}^{-1}$, which are in rough agreement with previous estimates in the region. Ice splinters caused drizzle drops to freeze on contact, forming additional instant-rimers. Larger drizzle and raindrops were preferentially frozen, as they were more likely to encounter splinters as a result of their larger size and fall speed.

960

 - Ice concentrations may have been enhanced by the release of shattered fragments as the larger drops froze. However, based on previous estimates of this process, this enhancement could only have been up to a maximum of $\sim 20\%$, and is unlikely to have caused the large increase in ice concentrations observed.

965

 - Frozen drizzle/raindrops and splinters were redistributed around the cloud by thermal circulation, and grew by riming and vapour deposition. Larger frozen drops formed millimetre-sized graupel, which added to the precipitation.

970

 - Glaciated stratiform regions were formed as a result of the maturing of the clouds as they moved downwind. The concentration of cloud droplets will have been reduced by entrainment and conversion to ice, although the relative fractions of cloud drops lost to each of these effects are unknown. Ice remaining in the H-M zone grew to form precipitation-sized aggregates of columns, but this took place more slowly than the freezing of supercooled drizzle. At higher altitudes the ice formed complex, mixed-habit ice particles, due to riming and growth by vapour deposition at temperatures with different dominant ice habits. Much of the ice measured in the mature, stratiform regions showed columnar features, suggesting H-M is likely to have been the dominant ice formation process at the end of ice formation. At higher altitudes the ice formed complex, mixed-habit ice particles, due to riming and growth by vapour deposition at temperatures with different dominant ice habits. Columns remaining in the H-M zone grew to form precipitation-sized aggregates, but this took place more slowly than the freezing of supercooled drizzle.

975

980

In the early stages of secondary ice development, the majority of precipitation-sized ice were frozen drizzle/raindrops, but their concentrations were much higher than the IN concentrations predicted by DeMott et al. (2010), suggesting they were liquid drops frozen by contact with ice splinters small ice crystals. Frozen drops initially dominated concentrations of larger ice crystals, while small ice splinters required time to grow by vapour deposition. It is not clear what fraction of

the small ice may have been produced by H-M or ice multiplication associated with the freezing of the drops.

990 ~~It is therefore clear that when H-M takes place in the presence of significant concentrations of drizzle drops, the freezing of drizzle provides a pathway not only to advance the onset of the H-M process, but to accelerate the formation of ice and precipitation when it is taking place.~~

It is however clear that the warm rain and secondary ice processes are intimately linked. H-M requires cloud drops of a certain size, and is accelerated by the presence of freezing drizzle/rain to form instant-rimers (Phillips et al., 2001). Ice multiplication processes associated with droplet freezing is
995 thought to be more prolific for larger drops (Lawson et al., 2015). The young updrafts contained mostly cloud drops, whereas downdrafts and some updrafts at later stages contained fewer cloud drops but more ice and drizzle. Multiple thermals and cells emerged in a similar region over the measurement period, and the interaction between neighbouring cells and clouds can have a large impact in determining where and when different microphysical processes take place (Blyth and Latham,
1000 1997). While it is not in the scope of this paper to make a full analysis of the interaction between dynamics and microphysics, this is an important topic for future modelling studies to investigate.

One of the major challenges in analysing observations of convective clouds is the rapid timescale over which changes can occur. By making multiple penetrations spaced a few minutes apart through the same cloud region, we have generated a dataset that can be used to comment critically on model
1005 behaviour. For example, prototype versions of the Met Office Unified Model are being used to simulate this case at horizontal resolutions of 200 and 100 m (Leon et al., 2015). Such simulated cloud fields may be sampled with pseudo-aircraft penetrations such that the impact of changes to microphysical parameters or formulations can be identified (Abel and Shipway, 2007).

It has been known for some time that H-M can operate in warm-base convective clouds spanning
1010 the H-M temperature zone (e.g. Chisnell and Latham, 1976; Harris-Hobbs and Cooper, 1987; Blyth and Latham, 1993; Rangno and Hobbs, 2005) and that, by providing the initial graupel the freezing of supercooled drizzle/raindrops formed by the warm rain process can advance the onset of H-M (Phillips et al., 2001; Huang et al., 2008, 2011). The recent work by Lawson et al. (2015) suggests secondary ice production associated with droplet freezing may also be an important mechanism for
1015 cloud glaciation, but we are not able to fully quantify how much influence it had on the clouds in this study based on our observations alone. Our observations do show that the freezing of drizzle/raindrops is an important process that dominates the formation of large ice in the intermediate stages of cloud development. Based on the measured concentrations, we have postulated that the droplets must be frozen by contact with small ice particles, which may be produced by H-M, droplet freezing secondary ice production, or some hitherto unknown or underestimated mechanism. Further investigation of this process would require the use of a cloud probe capable of quantifying small ice concentrations in clouds with droplet concentrations up to several hundred per cubic centimetre.
1020 As these frozen drops were the first precipitation observed, it is clear that interactions between the

warm rain and secondary ice production processes are key to determining the timing and location of
1025 precipitation.

This work adds to the growing body of evidence (e.g. Chisnell and Latham, 1976; Harris-Hobbs and Cooper, 1987; Blyth and Latham, 1993; Rangno and Hobbs, 2005) suggesting that this interaction continues as H-M progresses, and is key to the rapid glaciation of the cloud. Drizzle/raindrops freeze by contact with splinters, and then act as instant rimers to create additional splinters, accelerating
1030 glaciation and the formation of ice-phase precipitation.

It has been suggested that the shattering of droplets upon freezing may also contribute to ice multiplication, particularly in tropical storms (Rangno and Hobbs, 2005; Lawson et al., 2015), though the laboratory-based evidence of this process is more limited. Our results suggest that in storms in the temperate zone, the warm rain process is active enough to accelerate H-M, but not for
1035 droplet-shattering to be a major source of ice. Accurate representation of both the H-M and warm rain processes, as well as their interactions with each other and cloud dynamics, appears key to making quantitative forecasts of the timing and location of precipitation.

Appendix A

A1 OAP data processing

1040 OAP data processing was performed to derive size- and shape-segregated number concentrations as in Crosier et al. (2011, 2014). The OAP data processing software uses the raw image data to derive size-segregated concentrations. The sample volume was calculated using the measured airspeed and size-dependent sample area, as described by Heymsfield and Parrish (1978). Several criteria were used to quality-assure the single-particle images. Particles with short inter-arrival times (IATs) are
1045 likely to be a result of ice shattering on the OAP inlet (Field et al., 2006), and those with IAT $< 10^{-6}$ s were rejected. Anti-shatter tips (Korolev et al., 2011) were also used to minimise this issue. The use of a flat IAT threshold can result in inadequate removal of shattering artefacts (Korolev and Field, 2015), and/or inappropriate filtering of real particles. Using either no IAT threshold, or a threshold of 2×10^{-6} s, caused a 5 – 15% increase, or decrease respectively, in the ice and round
1050 concentrations reported by the 2DS. Varying the IAT threshold had little effect on the derived ice and drizzle concentrations. The reported concentration of small drops was more affected, but this is not used in this analysis. Poorly-imaged particles with $< 80\%$ of the pixels filled within the image perimeter, and streaks (images 1-pixel wide due to a faulty pixel in the OAP array) > 5 pixels long were also rejected.
1055 The 2DS images were classified into different categories, shown in Table A1. Particles with area < 50 pixels were classed as small (S), and no shape analysis was performed on these particles, though they are likely to be liquid cloud drops. Those with area > 50 pixels are classified based on their circularity, and labelled low, medium and high irregularity (LI, MI and HI respectively). The

threshold of 50 pixels is larger than that used by Crosier et al. (2011), but results in more reliable
1060 shape classification. In this analysis, 50 pixels corresponded to a mean size of $\sim 90 \mu\text{m}$.

Visual inspection of the images showed that particles classed as LI were almost all round, and those classed as HI were almost all ice. Images in the MI category varied, and many were of indeterminate phase. The MI category was therefore divided proportionally between the LI and HI categories, to make new categories round and ice. [Varying the circularity thresholds \(in all categories concurrently\) by \$\pm 0.05\$ caused a 5 – 20 % change in the ice and round concentrations reported by the 2DS.](#) It was not possible to perform shape analysis on images overlapping the edge of the array, and those with area > 50 pixels (EL) were assigned to either the round or ice categories on a run-by-run basis. In practice, the edge particles were rarely mixed-phase, being either almost all round or almost all ice. The sample volume was calculated using the 'centre-in' approach (Heymsfield and Parrish, 1978). When combining the size distributions from the CDP, 2DS and CIP100 to calculate
1065
1070 the effective radius, the all-accept category was used for the OAPs.

Due to the high cloud drop concentrations encountered during COPE, the 2DS probe was occasionally overloaded with data, resulting in significant deadtime. This deadtime was calculated based on instrument diagnostics, and used to correct the instrument sample volume and therefore the derived number concentrations. In extreme cases, the deadtime approached 90% of the sample time
1075 over a 1 s interval. [The 2DS has two data channels measured by vertically- and horizontally-aligned detectors. We combined images from channels to calculate an average concentration. This technique improves the counting statistics in low concentrations, as the large majority of particles are observed only on a single channel.](#)

Table A1. Summary of 2DS data products. Level 1 refers to standard products output by the data processing software, and are mutually exclusive (i.e. any accepted particle falls into only one level 1 category). Level 2 products are specific to COPE. Particles with $IAT < 1 \mu s$ were excluded in all categories to minimise shattering artefacts.

2DS data products					
Level 1					
Category	Abbreviation	Area (pixels)	Circularity	Edge rejection	
Small	S	< 50	All	On	
Low irregularity	LI	≥ 50	< 1.2	On	
Medium irregularity	MI	≥ 50	$1.2 - 1.4$	On	
High irregularity	HI	≥ 50	> 1.4	On	
Edge small	ES	< 50	All	Only edge	
Edge large	EL	≥ 50	All	Only edge	
Level 2					
Category	Abbreviation	Calculation			
Large enough to be classified by shape	D90	LI + MI + HI + EL			
Round	-	LI + MI*LI/(LI+HI) [+EL] ^a			
Ice	-	LI + MI*HI/(LI+HI) [+EL] ^a			
All-Accept	-	S + LI + MI + HI + ES + EL			

^aEL particles were assigned to either the round or ice categories by visually examining the images on a run-by-run basis.

1080 A2 Ice production rate calculations

Harris-Hobbs and Cooper (1987) detailed a method to calculate the ice production rate required to sustain a population of ice in a given size range, assuming a system in a steady state with a constant ice growth rate. The inferred ice production rate (P_0) is calculated as

$$P_0 = [C(L_2) - C(L_1)] / t_{21}, \quad (\text{A1})$$

1085 where $C(L_i)$ is the measured concentration of ice particles smaller than L_i , and t_{21} is the time required for an ice crystal to grow via vapour deposition from size L_1 to L_2 .

t_{21} may be calculated using

$$t_{21} = (L_2 - L_1) / G(T), \quad (\text{A2})$$

where $G(T)$ is the ice growth rate as a function of temperature.

1090 We use values of $G(T)$ taken from Ryan et al. (1976) using the measurement temperature. The calculation assumes ice crystal growth at water saturation, which is valid in mixed-phase clouds,

but does not take into account growth by riming. Ryan et al. (1976) provided values of $G(T)$ for pristine columns and plates, but the appropriate crystal growth rates are unclear for irregular ice such as graupel. We therefore only apply the calculation in regions where columns comprise the
1095 large majority ice crystals. The accuracy of the derived values of P_0 is difficult to quantify, but is likely to be within an order of magnitude. For this analysis, we calculate P_0 using the cumulative ice size distribution smaller than 100 μm and smaller than 150 μm . The ice concentrations were calculated as described in Appendix A.

Acknowledgements. The authors wish to thank all those involved in COPE. The BAe-146-301 Atmospheric
1100 Research Aircraft was flown by Directflight Ltd and managed by the Facility for Airborne Atmospheric Measurements (FAAM), which is a joint entity of the Natural Environment Research Council (NERC) and the Met Office. Processed data are available from the British Atmospheric Data Centre. Raw data are archived at the University of Manchester and available on request. COPE was supported by NERC under grant numbers NE/J022594/1 and NE/J023507/1, and the Met Office funded the operation of the BAe-146 FAAM aircraft. The
1105 US investigators were funded by NSF grant AGS-1230203, and the UWKA was funded by NSF grant ATM-0832637. We would also like to thank David Leon for his technical comments which aided the preparation of the manuscript.

References

- Abel, S. J. and Shipway, B. J.: A comparison of cloud-resolving model simulations of trade wind cumulus
1110 with aircraft observations taken during RICO, *Quarterly Journal of the Royal Meteorological Society*, 133,
781–794, doi:10.1002/qj.55, <http://doi.wiley.com/10.1002/qj.55>, 2007.
- Baumgardner, D., Jonsson, H., Dawson, W., O'Connor, D., and Newton, R.: The cloud, aerosol
and precipitation spectrometer: a new instrument for cloud investigations, *Atmospheric Research*,
59-60, 251–264, doi:10.1016/S0169-8095(01)00119-3, <http://www.sciencedirect.com/science/article/pii/S0169809501001193>, 2001.
- Baumgardner, D., Popovicheva, O., Allan, J., Bernardoni, V., Cao, J., Cavalli, F., Cozic, J., Diapouli, E., Eleftheriadis, K., Genberg, P. J., Gonzalez, C., Gysel, M., John, A., Kirchstetter, T. W., Kuhlbusch, T. A. J.,
1115 Laborde, M., Lack, D., Müller, T., Niessner, R., Petzold, A., Piazzalunga, A., Putaud, J. P., Schwarz, J., Sheridan, P., Subramanian, R., Swietlicki, E., Valli, G., Vecchi, R., and Viana, M.: Soot reference materials
for instrument calibration and intercomparisons: a workshop summary with recommendations, *Atmospheric
Measurement Techniques*, 5, 1869–1887, doi:10.5194/amt-5-1869-2012, <http://www.atmos-meas-tech.net/5/1869/2012/amt-5-1869-2012.html>, 2012.
- Bennett, L. J., Browning, K. A., Blyth, A. M., Parker, D. J., and Clark, P. A.: A review of the initiation of
precipitating convection in the United Kingdom, *Quarterly Journal of the Royal Meteorological Society*,
1120 132, 1001–1020, doi:10.1256/qj.05.54, <http://doi.wiley.com/10.1256/qj.05.54>, 2006.
- Beswick, K. M., Gallagher, M. W., Webb, A. R., Norton, E. G., and Perry, F.: Application of the Aventech AIMMS20AQ airborne probe for turbulence measurements during the Convective Storm Initiation Project, *Atmospheric Chemistry and Physics*, 8, 5449–5463, doi:10.5194/acp-8-5449-2008, <http://www.atmos-chem-phys.net/8/5449/2008/acp-8-5449-2008.html>, 2008.
- Blyth, A. M. and Latham, J.: Development of ice and precipitation in New Mexican summertime cumulus
1130 clouds, *Quarterly Journal of the Royal Meteorological Society*, 119, 91–120, doi:10.1002/qj.49711950905,
<http://doi.wiley.com/10.1002/qj.49711950905>, 1993.
- Blyth, A. M. and Latham, J.: A multi-thermal model of cumulus glaciation via the hallett-Mossop process,
Quarterly Journal of the Royal Meteorological Society, 123, 1185–1198, doi:10.1002/qj.49712354104, http:
1135 //doi.wiley.com/10.1002/qj.49712354104, 1997.
- Blyth, A. M., Lasher-Trapp, S. G., and Cooper, W. A.: A study of thermals in cumulus clouds, *Quarterly Journal
of the Royal Meteorological Society*, 131, 1171–1190, doi:10.1256/qj.03.180, <http://doi.wiley.com/10.1256/qj.03.180>, 2005.
- Blyth, A. M., Bennett, L. J., and Collier, C. G.: High-resolution observations of precipitation from cumulonimbus
1140 clouds, *Meteorological Applications*, 22, 75–89, doi:10.1002/met.1492, <http://doi.wiley.com/10.1002/met.1492>, 2015.
- Browning, K. A., Morcrette, C. J., Nicol, J., Blyth, A. M., Bennett, L. J., Brooks, B. J., Marsham, J., Mobbs,
S. D., Parker, D. J., Perry, F., Clark, P. A., Ballard, S. P., Dixon, M. A., Forbes, R. M., Lean, H. W., Li, Z.,
Roberts, N. M., Corsmeier, U., Barthlott, C., Deny, B., Kalthoff, N., Khodayar, S., Kohler, M., Kottmeier,
1145 C., Kraut, S., Kunz, M., Lenfant, J., Wieser, A., Agnew, J. L., Bamber, D., McGregor, J., Beswick, K. M.,
Gray, M. D., Norton, E., Ricketts, H. M. A., Russell, A., Vaughan, G., Webb, A. R., Bitter, M., Feuerle, T.,
Hankers, R., Schulz, H., Bozier, K. E., Collier, C. G., Davies, F., Gaffard, C., Hewison, T. J., Ladd, D. N.,

- Slack, E. C., Waight, J., Ramatschi, M., Wareing, D. P., and Watson, R. J.: The Convective Storm Initiation Project, *Bulletin of the American Meteorological Society*, 88, 1939–1955, doi:10.1175/BAMS-88-12-1939,
 1150 <http://journals.ametsoc.org/doi/abs/10.1175/BAMS-88-12-1939>, 2007.
- Burpee, R. W.: Peninsula-Scale Convergence in the South Florida Sea Breeze, *Monthly Weather Review*, 107, 852–860, doi:10.1175/1520-0493(1979)107<0852:PSCITS>2.0.CO;2, [http://journals.ametsoc.org/doi/abs/10.1175/1520-0493\(1979\)107%3C0852%3APSCITS%3E2.0.CO%3B2](http://journals.ametsoc.org/doi/abs/10.1175/1520-0493(1979)107%3C0852%3APSCITS%3E2.0.CO%3B2), 1979.
- Canagaratna, M. R., Jayne, J. T., Jimenez, J. L., Allan, J. D., Alfarra, M. R., Zhang, Q., Onasch, T. B., Drewnick,
 1155 F., Coe, H., Middlebrook, A., Delia, A., Williams, L. R., Trimborn, A. M., Northway, M. J., DeCarlo, P. F., Kolb, C. E., Davidovits, P., and Worsnop, D. R.: Chemical and microphysical characterization of ambient aerosols with the aerodyne aerosol mass spectrometer., *Mass spectrometry reviews*, 26, 185–222, doi:10.1002/mas.20115, <http://www.ncbi.nlm.nih.gov/pubmed/17230437>, 2007.
- Chisnell, R. F. and Latham, J.: Ice particle multiplication in cumulus clouds, *Quarterly Journal of the Royal Meteorological Society*, 102, 133–156, doi:10.1002/qj.49710243111, <http://doi.wiley.com/10.1002/qj.49710243111>, 1976.
- Connolly, P. J., Flynn, M. J., Ulanowski, Z., Choularton, T. W., Gallagher, M. W., and Bower, K. N.: Calibration of the Cloud Particle Imager Probes Using Calibration Beads and Ice Crystal Analogs: The Depth of Field, *Journal of Atmospheric and Oceanic Technology*, 24, 1860–1879, doi:10.1175/JTECH2096.1,
 1165 <http://journals.ametsoc.org/doi/abs/10.1175/JTECH2096.1>, 2007.
- Cornwall Council: Preliminary Flood Risk Assessment Report, <http://www.cornwall.gov.uk/environment-and-planning/countryside/estuaries-rivers-and-wetlands/flood-risk/preliminary-flood-risk-assessment-2011/>, 2011.
- Crawford, I., Bower, K. N., Choularton, T. W., Dearden, C., Crosier, J., Westbrook, C., Capes, G., Coe, H.,
 1170 Connolly, P. J., Dorsey, J. R., Gallagher, M. W., Williams, P., Trembath, J., Cui, Z., and Blyth, A.: Ice formation and development in aged, wintertime cumulus over the UK: observations and modelling, *Atmospheric Chemistry and Physics*, 12, 4963–4985, doi:10.5194/acp-12-4963-2012, <http://www.atmos-chem-phys.net/12/4963/2012/acp-12-4963-2012.html>, 2012.
- Crosier, J., Bower, K. N., Choularton, T. W., Westbrook, C. D., Connolly, P. J., Cui, Z. Q., Crawford, I. P., Capes, G. L., Coe, H., Dorsey, J. R., Williams, P. I., Illingworth, A. J., Gallagher, M. W., and Blyth, A. M.: Observations of ice multiplication in a weakly convective cell embedded in supercooled mid-level stratus, *Atmospheric Chemistry and Physics*, 11, 257–273, doi:10.5194/acp-11-257-2011, <http://www.atmos-chem-phys.net/11/257/2011/acp-11-257-2011.html>, 2011.
- Crosier, J., Choularton, T. W., Westbrook, C. D., Blyth, A. M., Bower, K. N., Connolly, P. J., Dearden, C.,
 1180 Gallagher, M. W., Cui, Z., and Nicol, J. C.: Microphysical properties of cold frontal rainbands, *Quarterly Journal of the Royal Meteorological Society*, 140, 1257–1268, doi:10.1002/qj.2206, <http://doi.wiley.com/10.1002/qj.2206>, 2014.
- Dasari, H. P. and Salgado, R.: Numerical modelling of heavy rainfall event over Madeira Island in Portugal: sensitivity to different micro physical processes, *Meteorological Applications*, 22, 113–127, doi:10.1002/met.1375, <http://doi.wiley.com/10.1002/met.1375>, 2015.
- DeMott, P. J., Prenni, A. J., Liu, X., Kreidenweis, S. M., Petters, M. D., Twohy, C. H., Richardson, M. S., Eidhammer, T., and Rogers, D. C.: Predicting global atmospheric ice nuclei distributions and their impacts on

- climate., Proceedings of the National Academy of Sciences of the United States of America, 107, 11 217–22, doi:10.1073/pnas.0910818107, <http://www.pnas.org/content/early/2010/06/01/0910818107.abstract>, 2010.
- 1190 Drewnick, F., Hings, S. S., DeCarlo, P., Jayne, J. T., Gonin, M., Fuhrer, K., Weimer, S., Jimenez, J. L., Demerjian, K. L., Borrmann, S., and Worsnop, D. R.: A New Time-of-Flight Aerosol Mass Spectrometer (TOF-AMS)- Instrument Description and First Field Deployment, *Aerosol Science and Technology*, 39, 637–658, doi:10.1080/02786820500182040, <http://dx.doi.org/10.1080/02786820500182040>, 2005.
- Environment Agency: Flooding in England: A National Assessment of Flood Risk, Tech. rep., Environment
1195 Agency, Bristol, United Kingdom, https://www.gov.uk/government/uploads/system/uploads/attachment_data/file/292928/geho0609bqds-e-e.pdf, 2009.
- Field, P. R., Heymsfield, A. J., and Bansemer, A.: Shattering and Particle Interarrival Times Measured by Optical Array Probes in Ice Clouds, *Journal of Atmospheric and Oceanic Technology*, 23, 1357–1371, doi:10.1175/JTECH1922.1, <http://journals.ametsoc.org/doi/abs/10.1175/JTECH1922.1>, 2006.
- 1200 French, J. R., Vali, G., and Kelly, R. D.: Evolution of small cumulus clouds in Florida: observations of pulsating growth, *Atmospheric Research*, 52, 143–165, doi:10.1016/S0169-8095(99)00024-1, <http://www.sciencedirect.com/science/article/pii/S0169809599000241>, 1999.
- Golding, B., ed.: Boscastle and north Cornwall post flood event study—meteorological analysis of the conditions leading to flooding on 16 August 2004, 459, Met Office, <http://www.metoffice.gov.uk/media/pdf/m/g/FRTR459.pdf>, 2005.
- 1205 Golding, B., Clark, P., and May, B.: The Boscastle flood: Meteorological analysis of the conditions leading to flooding on 16 August 2004, *Weather*, 60, 230–235, doi:10.1256/wea.71.05, <http://doi.wiley.com/10.1256/wea.71.05>, 2005.
- Griggs, D. J. and Choularton, T. W.: A laboratory study of secondary ice particle production by the fragmentation of rime and vapour-grown ice crystals, *Quarterly Journal of the Royal Meteorological Society*, 112, 149–163, doi:10.1002/qj.49711247109, <http://doi.wiley.com/10.1002/qj.49711247109>, 1986.
- Hallett, J. and Mossop, S. C.: Production of secondary ice particles during the riming process, *Nature*, 249, 26–28, doi:10.1038/249026a0, <http://dx.doi.org/10.1038/249026a0>, 1974.
- Hand, W. H., Fox, N. I., and Collier, C. G.: A study of twentieth-century extreme rainfall events
1210 in the United Kingdom with implications for forecasting, *Meteorological Applications*, 11, 15–31, doi:10.1017/S1350482703001117, <http://doi.wiley.com/10.1017/S1350482703001117>, 2004.
- Harris-Hobbs, R. L. and Cooper, W. A.: Field Evidence Supporting Quantitative Predictions of Secondary Ice Production Rates, *Journal of the Atmospheric Sciences*, 44, 1071–1082, doi:10.1175/1520-0469(1987)044<1071:FESQPO>2.0.CO;2, <http://journals.ametsoc.org/doi/abs/10.1175/1520-0469%281987%29044%3C1071%3AFESQPO%3E2.0.CO%3B2>, 1987.
- 1215 Hering, S. V., Stolzenburg, M. R., Quant, F. R., Oberreit, D. R., and Keady, P. B.: A Laminar-Flow, Water-Based Condensation Particle Counter (WCPC), *Aerosol Science and Technology*, 39, 659–672, <http://www.tandfonline.com/doi/abs/10.1080/02786820500182123>, 2005.
- Heymsfield, A. J. and Parrish, J. L.: A Computational Technique for Increasing the Effective Sampling Volume of the PMS Two-Dimensional Particle Size Spectrometer, *Journal of Applied Meteorology*, 17, 1566–1572, doi:10.1175/1520-0450(1978)017<1566:ACTFIT>2.0.CO;2, [http://journals.ametsoc.org/doi/abs/10.1175/1520-0450\(1978\)017%3C1566%3AACTFIT%3E2.0.CO%3B2](http://journals.ametsoc.org/doi/abs/10.1175/1520-0450(1978)017%3C1566%3AACTFIT%3E2.0.CO%3B2), 1978.

- Huang, X. F., Gao, R. S., Schwarz, J. P., He, L. Y., Fahey, D. W., Watts, L. A., McComiskey, A., Cooper, O. R., Sun, T. L., Zeng, L. W., Hu, M., and Zhang, Y. H.: Black carbon measurements in the Pearl River Delta
1230 region of China, *Journal of Geophysical Research-Atmospheres*, 116, doi:D12208 10.1029/2010jd014933,
2011.
- Huang, Y., Blyth, A. M., Brown, P. R. A., Choularton, T. W., Connolly, P., Gadian, A. M., Jones, H., Latham, J.,
Cui, Z., and Carslaw, K.: The development of ice in a cumulus cloud over southwest England, *New Journal
1235 of Physics*, 10, 105 021, doi:10.1088/1367-2630/10/10/105021, <http://stacks.iop.org/1367-2630/10/i=10/a=105021>, 2008.
- Koenig, L. R.: The Glaciating Behavior of Small Cumulonimbus Clouds, *Journal of the Atmospheric Sciences*, 20, 29–47, doi:10.1175/1520-0469(1963)020<0029:TGBOSC>2.0.CO;2, [http://journals.ametsoc.org/doi/abs/10.1175/1520-0469\(1963\)020%3C0029%3ATGBOSC%3E2.0.CO%3B2](http://journals.ametsoc.org/doi/abs/10.1175/1520-0469(1963)020%3C0029%3ATGBOSC%3E2.0.CO%3B2), 1963.
- Korolev, A. and Field, P. R.: Assessment of the performance of the inter-arrival time algorithm to iden-
1240 tify ice shattering artifacts in cloud particle probe measurements, *Atmospheric Measurement Techniques*, 8, 761–777, doi:10.5194/amt-8-761-2015, <http://www.atmos-meas-tech.net/8/761/2015/amt-8-761-2015.html>, 2015.
- Korolev, A. and Sussman, B.: A Technique for Habit Classification of Cloud Particles, *Journal of Atmospheric and Oceanic Technology*, 17, 1048–1057, doi:10.1175/1520-0426(2000)017<1048:ATFHCO>2.0.CO;2,
1245 [http://journals.ametsoc.org/doi/abs/10.1175/1520-0426\(2000\)017<1048:ATFHCO>2.0.CO;2](http://journals.ametsoc.org/doi/abs/10.1175/1520-0426(2000)017<1048:ATFHCO>2.0.CO;2), 2000.
- Korolev, A. V., Bailey, M. P., Hallett, J., and Isaac, G. A.: Laboratory and In Situ Obser-
vation of Deposition Growth of Frozen Drops, *Journal of Applied Meteorology*, 43, 612–622,
doi:10.1175/1520-0450(2004)043<0612:LAISOO>2.0.CO;2, <http://journals.ametsoc.org/doi/full/10.1175/1520-0450%282004%29043%3C0612%3ALAISOO%3E2.0.CO%3B2>, 2004.
- 1250 Korolev, A. V., Emery, E. F., Strapp, J. W., Cober, S. G., Isaac, G. A., Wasey, M., and Marcotte, D.: Small
Ice Particles in Tropospheric Clouds: Fact or Artifact? Airborne Icing Instrumentation Evaluation Ex-
periment, *Bulletin of the American Meteorological Society*, 92, 967–973, doi:10.1175/2010BAMS3141.1,
<http://journals.ametsoc.org/doi/abs/10.1175/2010BAMS3141.1>, 2011.
- Laborde, M., Schnaiter, M., Linke, C., Saathoff, H., Naumann, K.-H., Möhler, O., Berlenz, S., Wagner,
1255 U., Taylor, J. W., Liu, D., Flynn, M., Allan, J. D., Coe, H., Heimerl, K., Dahlkötter, F., Weinzierl,
B., Wollny, A. G., Zanatta, M., Cozic, J., Laj, P., Hitzenberger, R., Schwarz, J. P., and Gysel, M.:
Single Particle Soot Photometer intercomparison at the AIDA chamber, *Atmospheric Measurement
Techniques*, 5, 3077–3097, doi:10.5194/amt-5-3077-2012, <http://www.atmos-meas-tech.net/5/3077/2012/amt-5-3077-2012.html>, 2012.
- 1260 Lance, S.: Coincidence Errors in a Cloud Droplet Probe (CDP) and a Cloud and Aerosol Spectrometer
(CAS), and the Improved Performance of a Modified CDP, *Journal of Atmospheric and Oceanic Tech-
nology*, 29, 1532–1541, doi:10.1175/JTECH-D-11-00208.1, <http://journals.ametsoc.org/doi/full/10.1175/JTECH-D-11-00208.1>, 2012.
- Lance, S., Brock, C. A., Rogers, D., and Gordon, J. A.: Water droplet calibration of the Cloud Droplet Probe
1265 (CDP) and in-flight performance in liquid, ice and mixed-phase clouds during ARCPAC, *Atmospheric
Measurement Techniques*, 3, 1683–1706, doi:10.5194/amt-3-1683-2010, <http://www.atmos-meas-tech.net/3/1683/2010/amt-3-1683-2010.html>, 2010.

- Lawson, R. P. and Cooper, W. A.: Performance of Some Airborne Thermometers in Clouds, *Journal of Atmospheric and Oceanic Technology*, 7, 480–494, doi:10.1175/1520-0426(1990)007<0480:POSATI>2.0.CO;2,
 1270 http://journals.ametsoc.org/doi/abs/10.1175/1520-0426(1990)007%3C0480%3APOSATI%3E2.0.CO%
 3B2, 1990.
- Lawson, R. P., O'Connor, D., Zmarzly, P., Weaver, K., Baker, B., Mo, Q., and Jonsson, H.: The 2D-S (Stereo) Probe: Design and Preliminary Tests of a New Airborne, High-Speed, High-Resolution Particle Imaging Probe, *Journal of Atmospheric and Oceanic Technology*, 23, 1462–1477, doi:10.1175/JTECH1927.1, http:
 1275 //journals.ametsoc.org/doi/full/10.1175/JTECH1927.1, 2006.
- Lawson, R. P., Woods, S., and Morrison, H.: The Microphysics of Ice and Precipitation Development in Tropical Cumulus Clouds, *Journal of the Atmospheric Sciences*, 72, 2429–2445, doi:10.1175/JAS-D-14-0274.1, http://journals.ametsoc.org/doi/abs/10.1175/JAS-D-14-0274.1, 2015.
- Leon, D., French, J. R., Lasher-Trapp, S. G., Blyth, A. M., Abel, S. J., Ballard, S., Bennett, L. J., Bower, K. N.,
 1280 Brooks, B. J., Brown, P., Choularton, T. W., Clark, P., Collier, C. G., Crosier, J., Cui, Z., Dufton, D., Eagle, C., Flynn, M. J., Gallagher, M., Hanley, K. E., Huang, Y., Kitchen, M., Korolev, A., Lean, H. W., Liu, Z., Marsham, J., Moser, D., Nichol, J., Norton, E., Plummer, D., Price, J., Ricketts, H. M. A., Taylor, J. W., Roberts, N. M., and Williams, P. I.: The COncective Precipitation Experiment (COPE): Investigating the origins of heavy precipitation in the southwestern UK, *Bulletin of the American Meteorological Society*,
 1285 Accepted, 2015.
- Loftus, A. and Cotton, W.: A triple-moment hail bulk microphysics scheme. Part II: Verification and comparison with two-moment bulk microphysics, *Atmospheric Research*, 150, 97–128, doi:10.1016/j.atmosres.2014.07.016, http://www.sciencedirect.com/science/article/pii/S0169809514002798, 2014.
- 1290 Mangia, C., Martano, P., Miglietta, M. M., Morabito, A., and Tanzarella, A.: Modelling local winds over the Salento peninsula, *Meteorological Applications*, 11, 231–244, doi:10.1017/S135048270400132X, http://doi.wiley.com/10.1017/S135048270400132X, 2004.
- Met Office: Met Office Rain Radar Data from the NIMROD System., http://catalogue.ceda.ac.uk/uuid/82adec1f896af6169112d09cc1174499, 2003.
- 1295 Mossop, S. C.: Production of secondary ice particles during the growth of graupel by riming, *Quarterly Journal of the Royal Meteorological Society*, 102, 45–57, doi:10.1002/qj.49710243104, http://doi.wiley.com/10.1002/qj.49710243104, 1976.
- Mossop, S. C.: The influence of drop size distribution on the production of secondary ice particles during graupel growth, *Quarterly Journal of the Royal Meteorological Society*, 104, 323–330,
 1300 doi:10.1002/qj.49710444007, http://doi.wiley.com/10.1002/qj.49710444007, 1978.
- Phillips, V. T. J., Blyth, A. M., Brown, P. R. A., Choularton, T. W., and Latham, J.: The glaciation of a cumulus cloud over New Mexico, *Quarterly Journal of the Royal Meteorological Society*, 127, 1513–1534, doi:10.1002/qj.49712757503, http://doi.wiley.com/10.1002/qj.49712757503, 2001.
- Rangno, A. L.: Fragmentation of Freezing Drops in Shallow Maritime Frontal Clouds, *Journal of the Atmospheric Sciences*, 65, 1455–1466, doi:10.1175/2007JAS2295.1, http://journals.ametsoc.org/doi/abs/10.1175/2007JAS2295.1, 2008.

- Rangno, A. L. and Hobbs, P. V.: Ice particles in stratiform clouds in the Arctic and possible mechanisms for the production of high ice concentrations, *Journal of Geophysical Research*, 106, 15 065, doi:10.1029/2000JD900286, <http://doi.wiley.com/10.1029/2000JD900286>, 2001.
- 1310 Rangno, A. L. and Hobbs, P. V.: Microstructures and precipitation development in cumulus and small cumulonimbus clouds over the warm pool of the tropical Pacific Ocean, *Quarterly Journal of the Royal Meteorological Society*, 131, 639–673, doi:10.1256/qj.04.13, <http://doi.wiley.com/10.1256/qj.04.13>, 2005.
- Rosenberg, P. D., Dean, A. R., Williams, P. I., Dorsey, J. R., Minikin, A., Pickering, M. A., and Petzold, A.: Particle sizing calibration with refractive index correction for light scattering optical particle counters and impacts upon PCASP and CDP data collected during the Fennec campaign, *Atmospheric Measurement Techniques*, 5, 1147–1163, doi:10.5194/amt-5-1147-2012, <http://www.atmos-meas-tech.net/5/1147/2012/amt-5-1147-2012.html>, 2012.
- 1315 Ryan, B. F., Wishart, E. R., and Shaw, D. E.: The Growth Rates and Densities of Ice Crystals between -3°C and -21°C, *Journal of the Atmospheric Sciences*, 33, 842–850, doi:10.1175/1520-0469(1976)033<0842:TGRADO>2.0.CO;2, <http://journals.ametsoc.org/doi/abs/10.1175/1520-0469%281976%29033%3C0842%3ATGRADO%3E2.0.CO%3B2>, 1976.
- Schwarz, J. P., Spackman, J. R., Gao, R. S., Perring, A. E., Cross, E., Onasch, T. B., Ahern, A., Wrobel, W., Davidovits, P., Olfert, J., Dubey, M. K., Mazzoleni, C., and Fahey, D. W.: The Detection Efficiency of the Single Particle Soot Photometer, *Aerosol Science and Technology*, 44, 612–628, 1320 doi:10.1080/02786826.2010.481298, <http://dx.doi.org/10.1080/02786826.2010.481298>, 2010.
- Stein, T. H. M., Hogan, R. J., Clark, P. A., Halliwell, C. E., Hanley, K. E., Lean, H. W., Nicol, J. C., and Plant, R. S.: The DYMECS project: A statistical approach for the evaluation of convective storms in high-resolution NWP models, *Bulletin of the American Meteorological Society*, p. 150212130411009, doi:10.1175/BAMS-D-13-00279.1, <http://journals.ametsoc.org/doi/abs/10.1175/BAMS-D-13-00279.1>, 2015.
- 1330 Stephens, M., Turner, N., and Sandberg, J.: Particle Identification by Laser-Induced Incandescence in a Solid-State Laser Cavity, *Appl. Opt.*, 42, 3726–3736, <http://ao.osa.org/abstract.cfm?URI=ao-42-19-3726>, 2003.
- Sun, J., Ariya, P. A., Leighton, H. G., and Yau, M. K.: Mystery of ice multiplication in warm-based precipitating shallow cumulus clouds, *Geophysical Research Letters*, 37, n/a–n/a, doi:10.1029/2010GL042440, <http://doi.wiley.com/10.1029/2010GL042440>, 2010.
- 1335 Wang, Y. and Geerts, B.: Estimating the Evaporative Cooling Bias of an Airborne Reverse Flow Thermometer, *Journal of Atmospheric and Oceanic Technology*, 26, 3–21, doi:10.1175/2008JTECHA1127.1, <http://journals.ametsoc.org/doi/full/10.1175/2008JTECHA1127.1>, 2009.
- Wang, Z., French, J., Vali, G., Wechsler, P., Haimov, S., Rodi, A., Deng, M., Leon, D., Snider, J., Peng, L., and Pazmany, A. L.: Single Aircraft Integration of Remote Sensing and In Situ Sampling for the 1340 Study of Cloud Microphysics and Dynamics, *Bulletin of the American Meteorological Society*, 93, 653–668, doi:10.1175/BAMS-D-11-00044.1, <http://journals.ametsoc.org/doi/abs/10.1175/BAMS-D-11-00044.1>, 2012.
- Warren, R. A., Kirshbaum, D. J., Plant, R. S., and Lean, H. W.: A ‘Boscawen-type’ quasi-stationary convective system over the UK Southwest Peninsula, *Quarterly Journal of the Royal Meteorological Society*, 140, 240–257, doi:10.1002/qj.2124, <http://doi.wiley.com/10.1002/qj.2124>, 2014.

Yano, J.-I. and Phillips, V. T. J.: Ice–Ice Collisions: An Ice Multiplication Process in Atmospheric Clouds, Journal of the Atmospheric Sciences, 68, 322–333, doi:10.1175/2010JAS3607.1, <http://journals.ametsoc.org/doi/abs/10.1175/2010JAS3607.1>, 2011.

Table 1. Mean and standard deviation of aerosol number and composition during a run along the peninsula at 570 m, between 11:52:14 – 11:58:53 UTC. The AMS chloride measurement ($\text{Chl}_{\text{NSS}}^-$) does not include sea salt, so the total chloride concentration is likely to have been higher. The s preceding the concentration units denotes that the data are corrected to standard temperature and pressure (273.15 K and 1013.25 hPa).

	Mean	Standard deviation	Number of data points	Instrument
Total aerosol conc. (scm^{-3})	6600	2900	399	CPC
Aerosol > 0.5 μm (scm^{-3})	5.0	2.4	399	PCASP/CDP
SO_4^{2-} ($\mu\text{g sm}^{-3}$)	1.62	0.22	13	AMS
NO_3^- ($\mu\text{g sm}^{-3}$)	0.10	0.05	13	AMS
NH_4^+ ($\mu\text{g sm}^{-3}$)	0.51	0.07	13	AMS
Org ($\mu\text{g sm}^{-3}$)	0.44	0.10	13	AMS
$\text{Chl}_{\text{NSS}}^-$ ($\mu\text{g sm}^{-3}$)	0.05	0.04	13	AMS
BC ($\mu\text{g sm}^{-3}$)	0.0176	0.074	399	SP2

Table 2. Summary of straight and level runs made by the BAe-146 shown in Figs. 5 – 12. The run numbers correspond to full or sections of labelled runs in the archived flight logs. 2DS edge particles were assigned to either the ice or round categories on a run-by-run basis. Updraft/downdraft regions are defined by vertical velocity in the upper/lower 15 percentiles of each run when the 2DS was recording data. The cloud top temperature was calculated by interpolating measurements of cloud top height, taken by the NCAS precipitation radar and UWKA radar/lidar, and converting to the measured temperature at that altitude. The DeMott et al. (2010) IN concentrations are calculated using the cloud top temperature, and corrected to the temperature and pressure at the altitude where the BAe-146 was sampling.

Run	Start time	End time	Distance along axis CD (km)	Heading ($^\circ$)	Run altitude (km)	Run T ($^\circ\text{C}$)	Cloud top altitude (km)	Cloud top T ($^\circ\text{C}$)	2DS Edge category	Mean updraft ice (L^{-1})	Mean downdraft ice (L^{-1})	Cloud top IN (L^{-1})
Longitudinal run												
11.2	13:34:55	13:40:30	14 – 61	48	3.5	-5	3.3 – 5.2	-4 to -15	Ice	N/A	N/A	0.007 – 0.9
Developing turret												
10.3	13:30:19	13:30:29	14 – 16	219	3.2	-3	3.4	-4	Round	0	0	0.0072
11.1	13:34:55	13:35:12	14 – 16	55	3.5	-5	3.7	-6	Round	0.19 ± 0.19^a	0.19 ± 0.19^a	0.022
11.4	13:49:08	13:49:54	19 – 24	197	3.5	-5	4.6	-12	Round	1.3	3.5	0.23
13	13:53:21	13:54:01	20 – 26	26	3.8	-7	4.9	-13	Round	0.24	0.94	0.33
14	13:58:01	13:58:39	24 – 28	191	4.1	-9	5.1	-14	Ice	15	38	0.45
15.1	14:02:05	14:02:46	26 – 31	4	4.4	-10	5.2	-15	Ice	42	34	0.52
15.2	14:04:28	14:05:10	25 – 27	164	4.4	-10	5.2	-15	Ice	20	96	0.55
16	14:10:04	14:10:37	31 – 33	342	4.7	-12	5.2	-15	Ice	107	69	0.50
Mature turret												
17.3	14:25:12	14:25:55	28 – 32	186	4.7	-12	5.4	-16	Ice	137	127	1.2

^a The errors listed are the Poisson counting errors, which are negligible for all other runs.

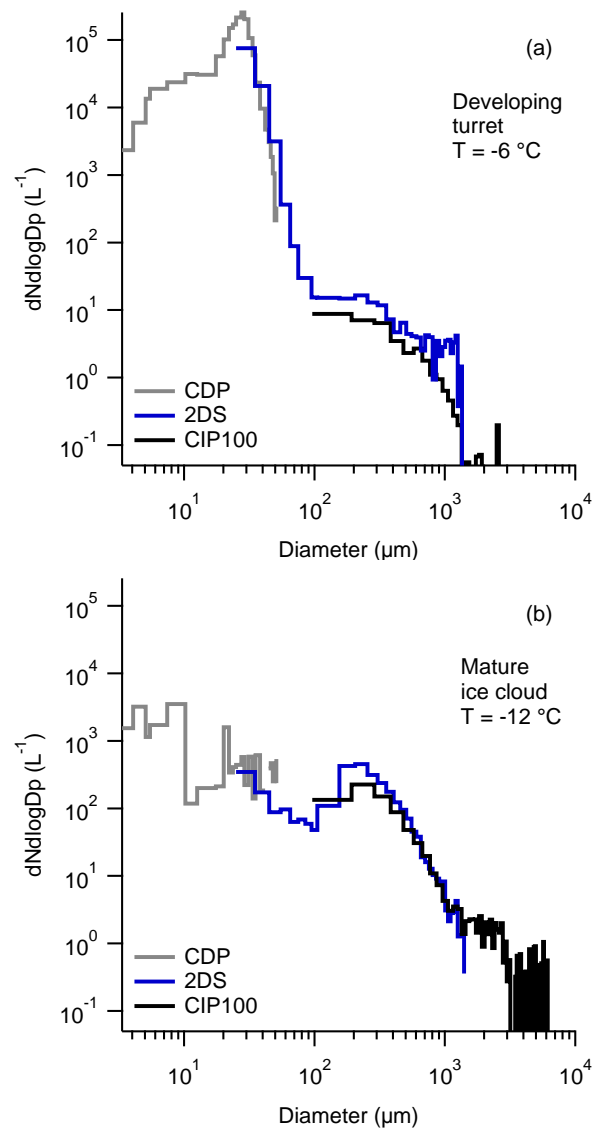


Figure 1. Comparison of size distributions from the CDP, 2DS and CIP100 probes during selected cloud penetrations through (a) a developing turret and (b) a mature glaciated region. The first 2 size bins from the 2DS and CIP100 were removed, as they are subject to large uncertainty, and are not used in this analysis.

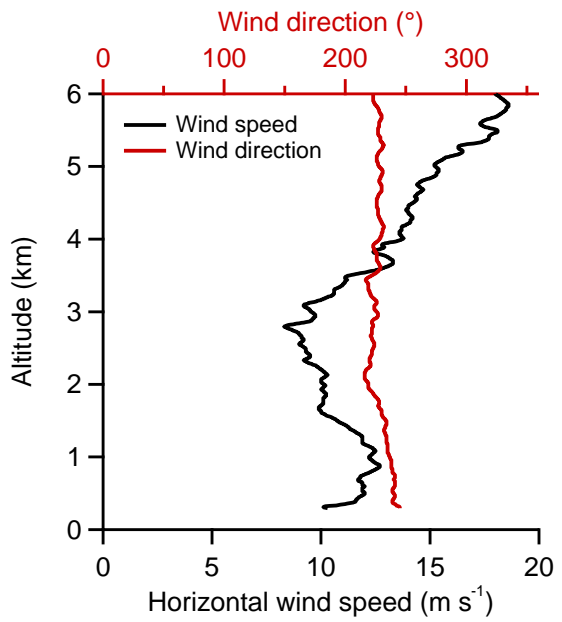


Figure 2. Vertical profile of horizontal wind speed and direction measured from the 1500 UTC radiosonde launched from Davidstow, the same location as the NCAS precipitation radar.

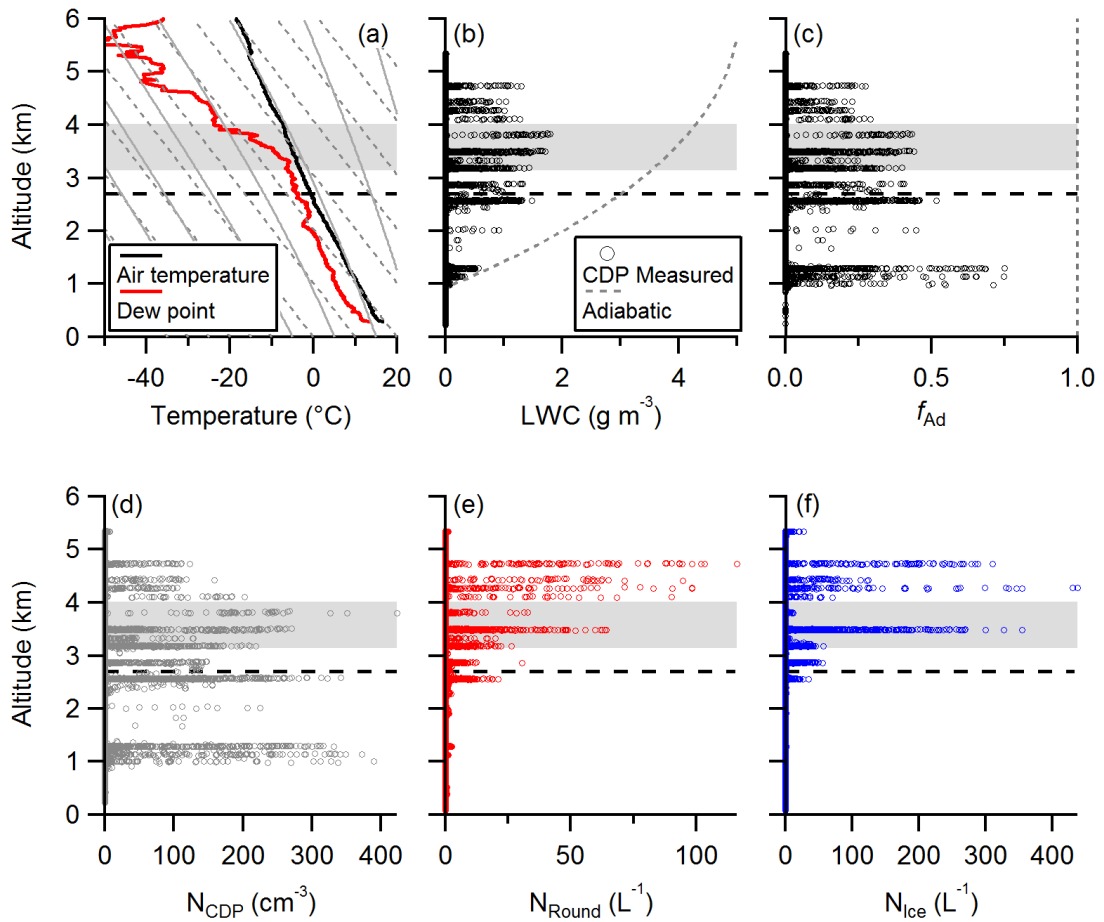


Figure 3. Vertical profile showing radiosonde data and cloud measurements made by the BAe-146. The horizontal dashed lines mark the 0°C level. Panel (a) shows temperature and dew point from the 1500 UTC radiosonde launched from Davidstow. The solid and dashed grey lines are wet pseudo adiabats and dry adiabats respectively, and the shaded region shows the H-M temperature zone. Panel (b) shows the LWC measured by the CDP, as well as the calculated adiabatic values. These data are converted to the adiabatic fraction, f_{Ad} in panel (c). Panel (d) shows the droplet concentration measured by the CDP, and panels (e) and (f) show the round and ice concentrations measured by the 2DS. In this plot only, edge particles measured by the 2DS are assigned to the round category for $T \geq 0^{\circ}\text{C}$, and the ice category elsewhere.

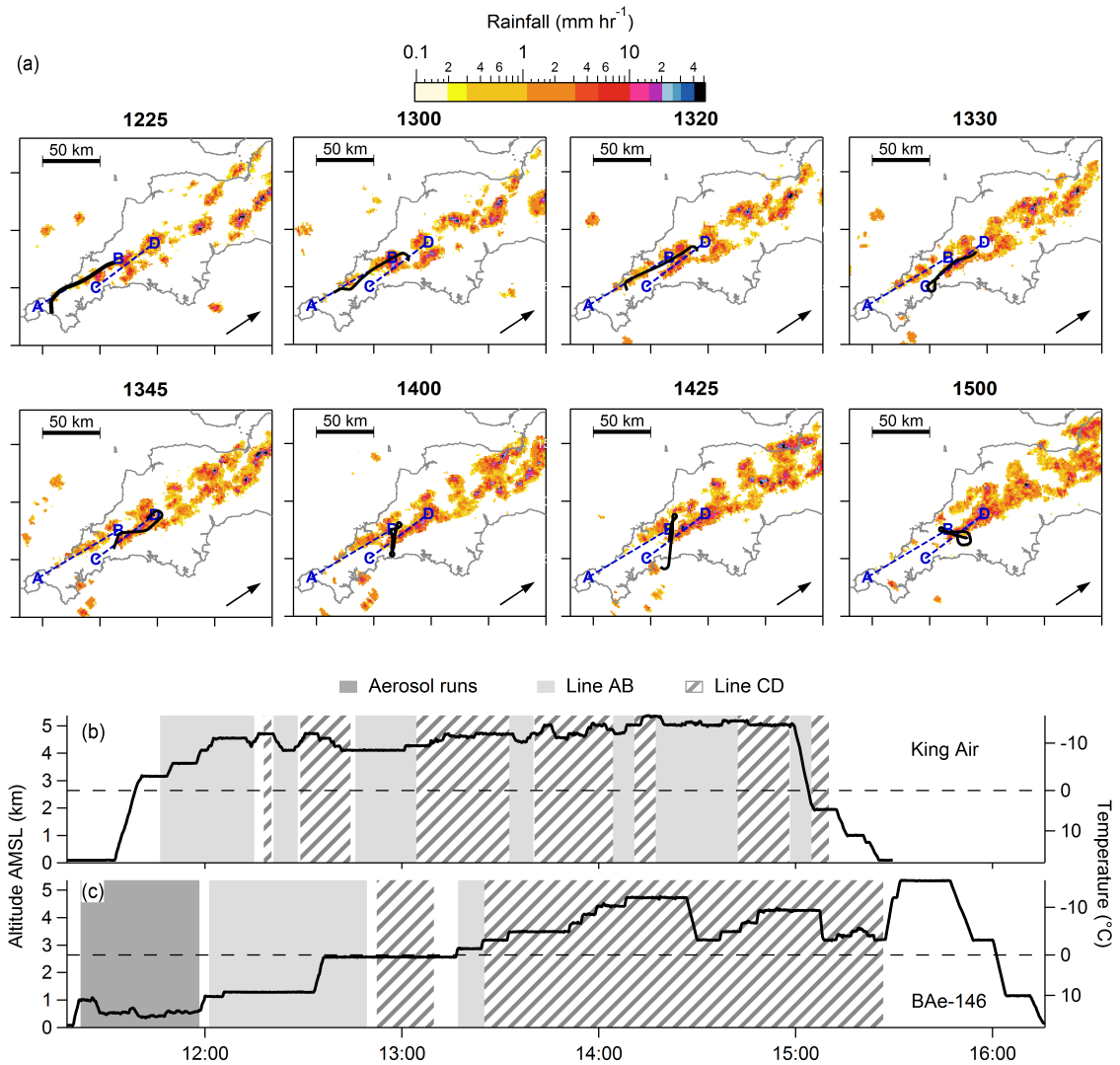


Figure 4. Overview of in situ cloud measurements made on 3rd August 2014. Panel (a) shows calculated precipitation from the UK operational radar network at several points during the afternoon. The blue dashed lines are axes AB and CD, and the black line is the flight track of the BAe-146 5 minutes either side of the time for each panel. The black arrow shows the wind direction. Panels (b) and (c) show time series of the altitude and sampling focus of the two aircraft. The listed times are in UTC, and the local time was UTC +1.

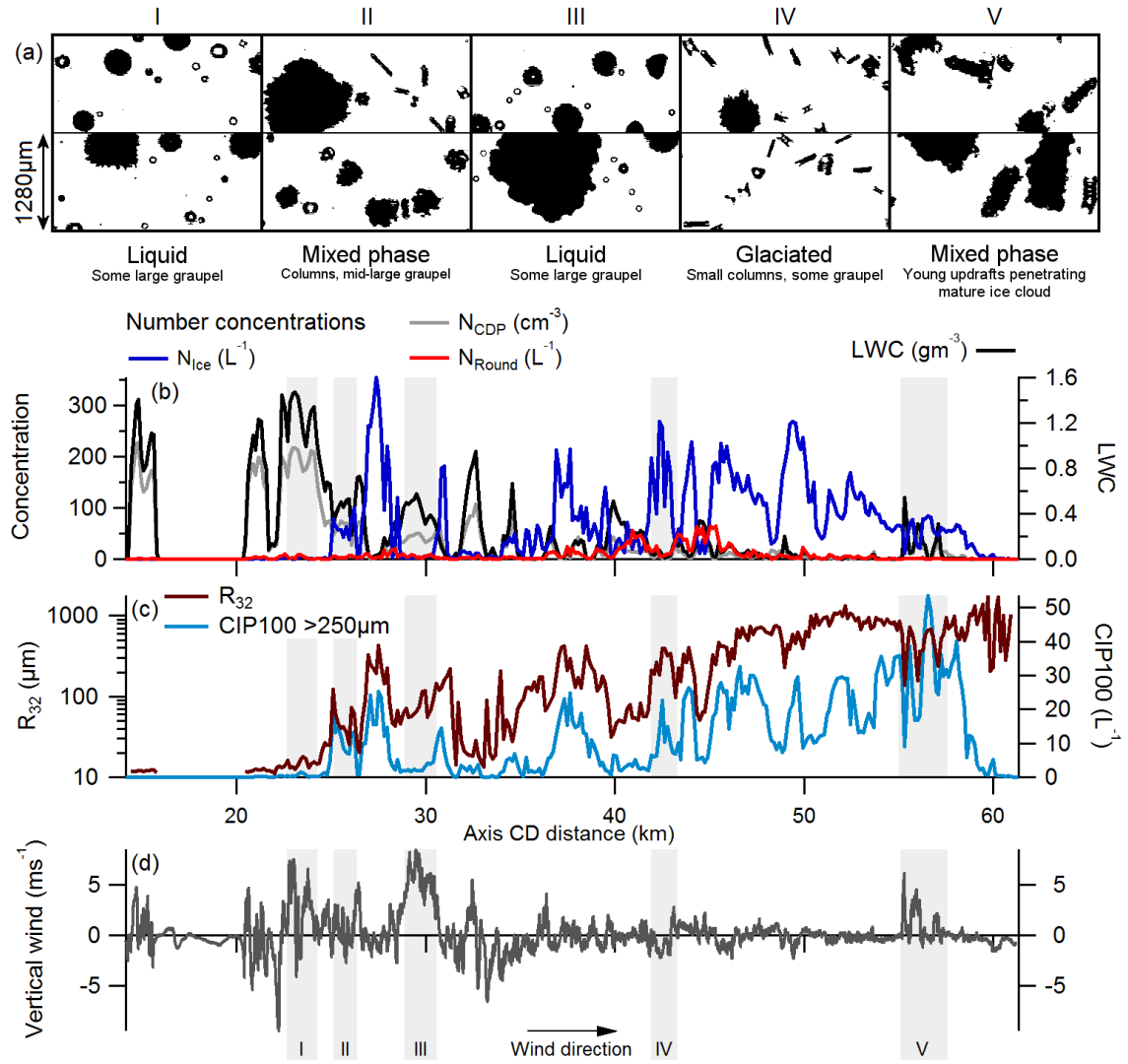


Figure 5. In situ measurements made by the BAe-146 on longitudinal Run 11.2 along axis CD. The run was made at an altitude of 3.5 km ($T \sim -5^\circ\text{C}$) between 13:34:55 and 13:40:30 UTC. In panel (b), the number concentrations use the left axis, and the units are defined according to the measurement probe. The 2DS categories are defined in Appendix A. The images shown were recorded by the 2DS and show representative images from the sections marked by grey boxes and labelled with Roman numerals. Only images >50 pixels are shown, and they are not classified by shape.

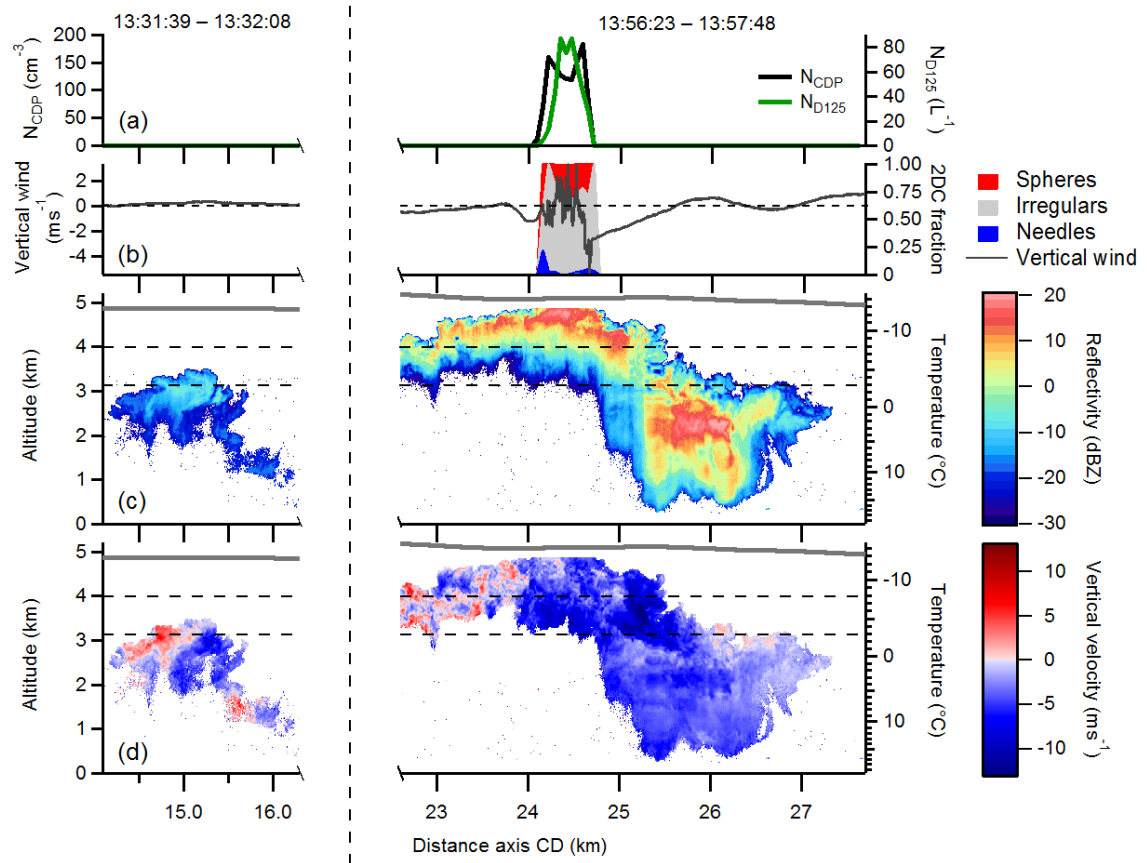


Figure 6. In situ and downward-pointing radar data measured aboard the UWKA during an overpass of a developing turret, and a penetration through the top of the same turret 25 minutes later. Panel (a) shows in situ concentrations N_{CDP} and N_{D125} , which was measured by the CIP25. Panel (b) shows the habit classifications of particles measured by the CIP25, and the in situ vertical wind velocity. The horizontal dashed line on panel (b) is the zero line for the vertical wind. Panels (c) and (d) show radar reflectivity and hydrometeor vertical velocity respectively. The horizontal dashed lines on panels (b) and (c) mark the H-M temperature zone, and the grey line shows the altitude the of the UWKA during the passes.

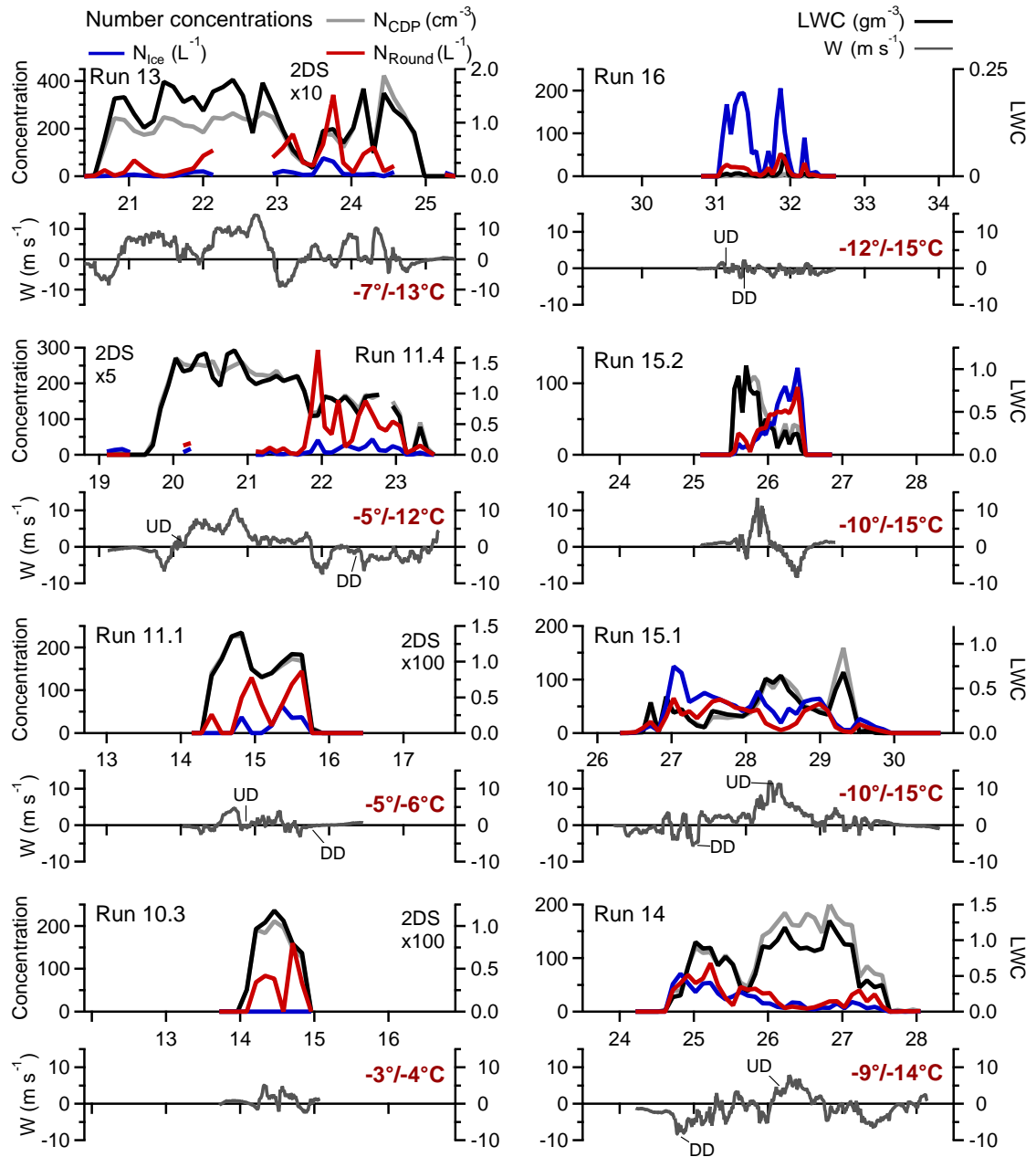


Figure 7. In situ data measured aboard the BAe-146 during a series of runs following an initially-isolated turret as it moved downwind, growing in height and glaciating as it spread to join the preceding line. The x-axis is the same as in Figs. 5 and 6. The colours of the traces shown are the same as in Fig. 5. For clarity, the 2DS traces (N_{Ice} and N_{Round}) in Runs 10.3 – 13 are multiplied by factors listed in the corresponding panel. The text in red shows the run temperature and the cloud top temperature. Further information for each run are listed in Table 2. For reference, concentrations during Run 16 would have been recorded 17% lower than those during Run 10.3 due to the change in temperature and pressure with altitude. The regions marked ‘UD’ and ‘DD’ show where the updraft and downdraft images in Figs. 8 and 9 are taken from.

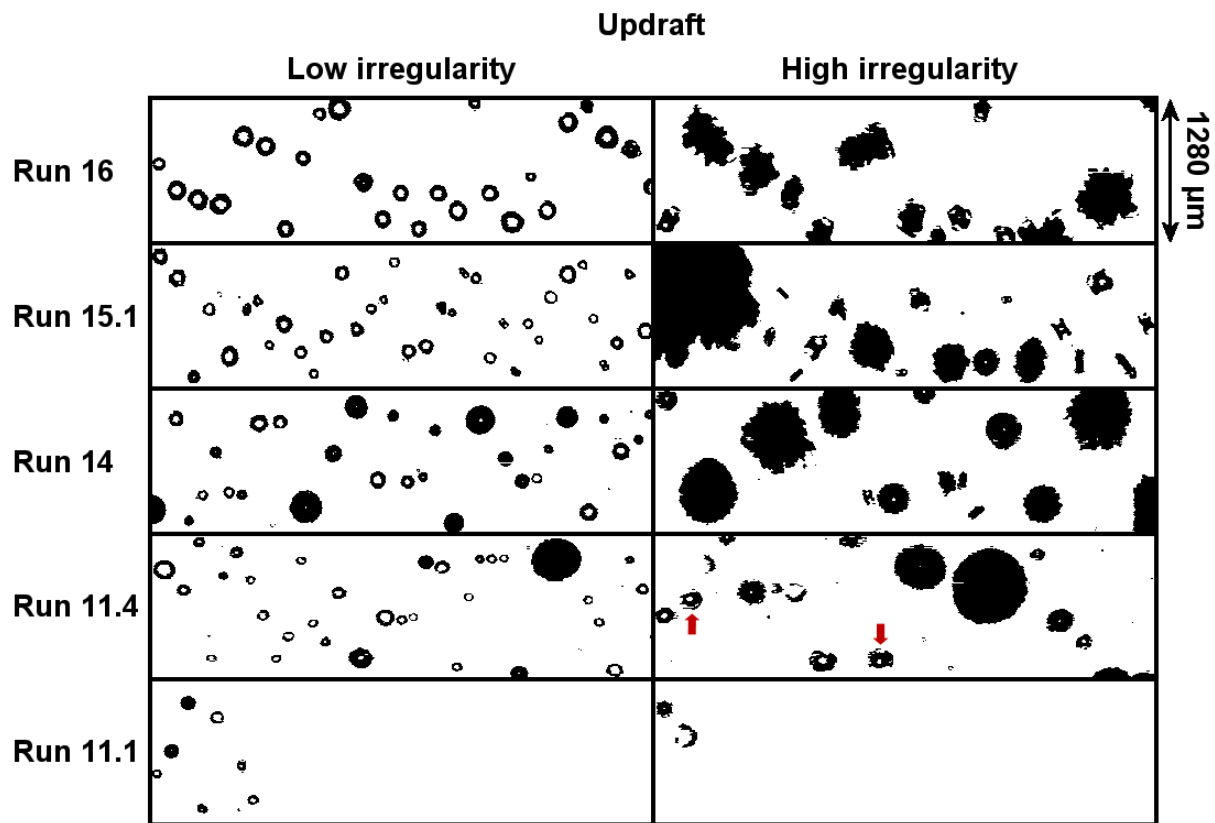


Figure 8. Images of hydrometeors measured by the 2DS during updrafts in selected runs from Fig. 7. Images with holes in the centre are out of focus. The images highlighted by red arrows are examples of frozen drops that may have also grown by vapour diffusion, as discussed in the text.

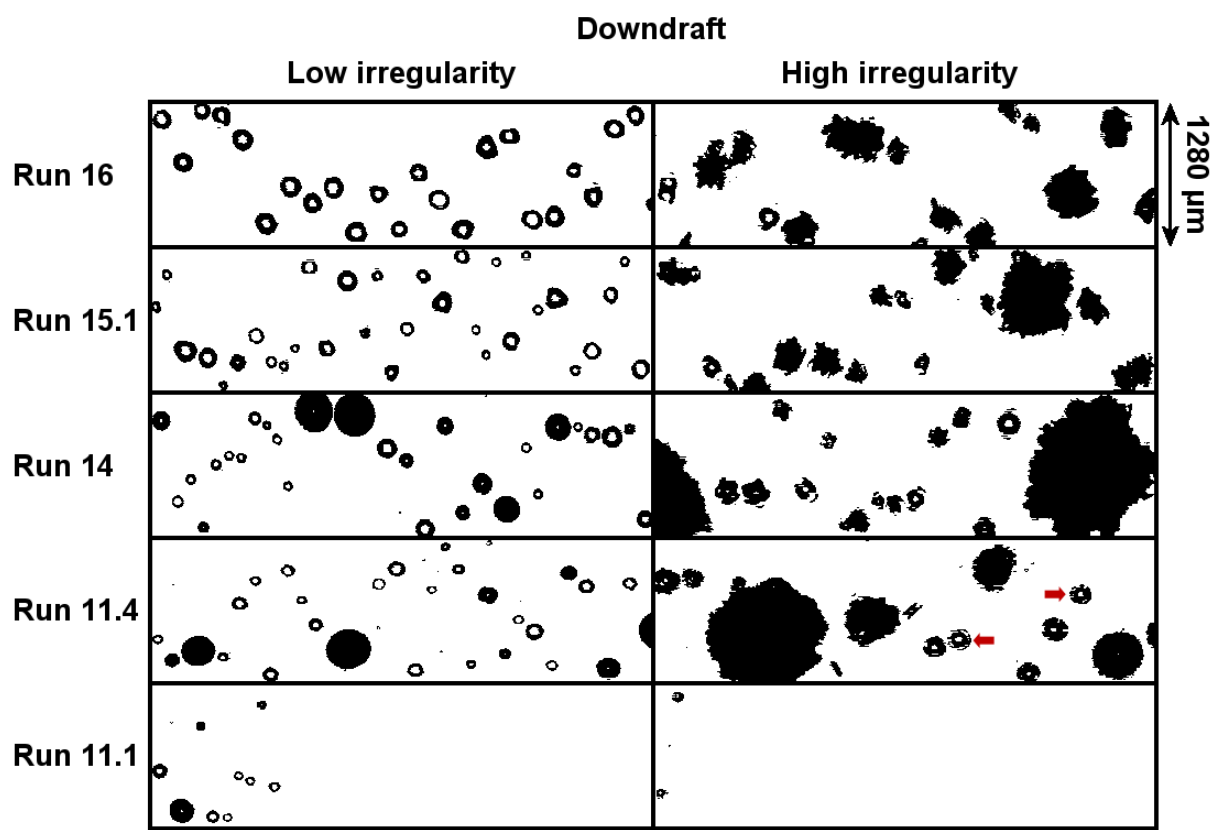


Figure 9. As Fig. 7, but for downdrafts.

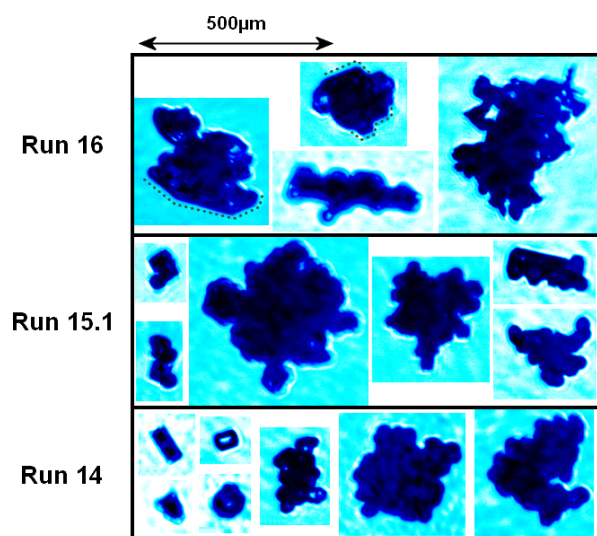


Figure 10. Images of hydrometeors measured by the CPI during selected runs from Fig. 7. Only a few images were recorded on each run, so they are not classified by vertical velocity. The dashed lines are to aid the reader's eye to the plate-like features, which may be difficult to see otherwise.

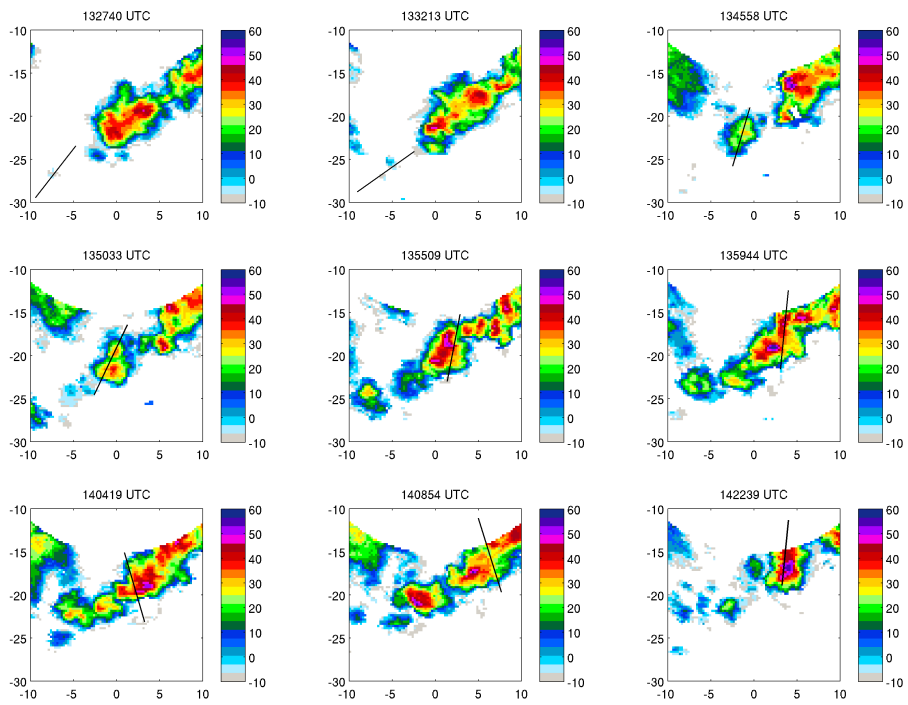


Figure 11. Radar reflectivity at 3.5 km altitude, measured by the NCAS precipitation radar during each of the runs shown in Fig. 7. The x and y axes are a Cartesian grid, showing kilometres East and West of the radar site, and the colourscale is in units of dBZ. 1 min of flight track is shown for each run.

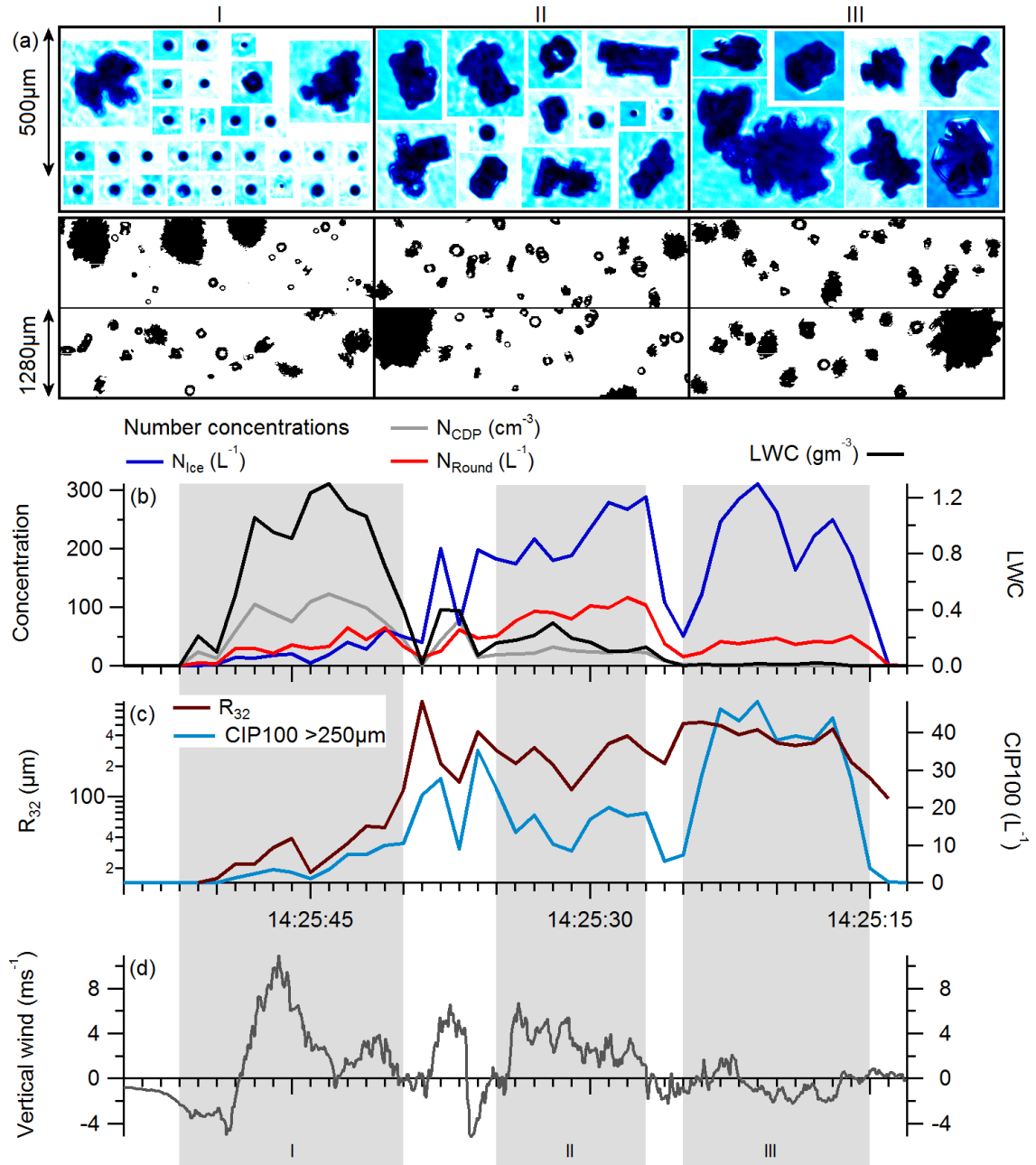


Figure 12. In situ measurements and images recorded by the BAe-146 probes during Run 17.3. The time axis runs backwards for clarity in the discussion. The images shown were recorded by the 2DS and CPI probes and are representative images of particles in the sections marked by grey boxes and labelled with Roman numerals. Only images >50 pixels are shown from the 2DS, and they are not classified by shape.

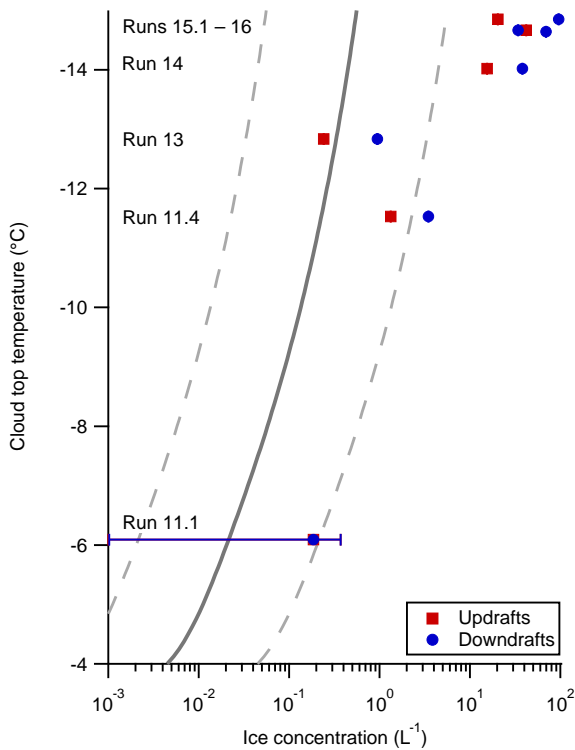


Figure 13. Mean ice concentrations measured during the runs in Figs. 7 – 11. The displayed errors are Poisson counting errors, which were negligible for all runs other than Run 11.1. The solid grey line is the IN concentration calculated using the DeMott et al. (2010) parametrisation, and the dashed grey lines are $10\times$ and $0.1\times$ the DeMott et al. values.